Integration of a Nuclear Rocket Engine onto a Lunar Hopper

Undergraduate Honors Research Thesis

Presented in Partial Fulfillment of the Requirements for Graduation with Distinction in the Department of Aerospace Engineering at The Ohio State University

November 18, 2019

Author

Michael J. Boazzo

Defense Committee

Dr. John M. Horack [Advisor]

Dr. Datta V. Gaitonde

Abstract

As human and robotic missions aim to establish a permanent presence on the Moon, there is a large economic and scientific incentive for the survey of the lunar surface for mineral deposits. The concept of a hopper is advantageous since roving can be impractical due to changing geography and uneven surfaces. Nuclear Thermal Propulsion (NTP) could be an ideal system to be integrated with a lunar hopper due to its high efficiency and dependency on a single propellant with a low atomic mass. The Moon has a low enough gravitational field that the thrust generated from an NTP engine will be high enough to lift mass off the surface and enter suborbital flight. In this paper we develop and articulate the concept of a lunar NTP hopper, a spacecraft that can land on the surface, take-off, and land again. These hops may potentially be repeated dozens of times due to the high thrust offered by the engine and maximize the number of landing sites. The goal of this paper was to find the range of possible solutions that will enable the lander to execute a simple set of design reference missions. While previous studies have focused on hypergolic propellants, the sole focus of this study is on NTP and integration onto a lunar testbed. Three different engines and dry mass combinations were tested among a list of possible mass ratios. A program in MATLAB was created so the optimum mass ratio, engine and dry mass combination could be highlighted. Upon reviewing the data, the Small Nuclear Reactor engine was selected with a target dry mass of 3500 kg. It was able to complete a total of 28, 16 and 8 hops for sub-orbital trajectories that were 5 km, 10, and 25 km in horizontal range.

Acknowledgements

This Undergraduate Thesis has been one of the greatest undertakings in my career as a student and an young engineer. I would personally like to thank, my advisor, Dr. John Horack for all his guidance, encouragement and selfless assistance not just with this project but for helping me shape the man I am today. I would also like to thank Dr. Elizabeth Newton, the director of the Battelle Center for Science, Engineering and Public Policy. She encouraged me to explore this largely unconsidered idea and to extend my graduation to pursue this vision and co-op opportunities at NASA Johnson Space Center. There were many times where I didn't know where to even begin or where I was stuck without a clear path forward. I would personally like to thank all the people who took time out of their busy schedules to help me conquer all the obstacles I had to face. From fixing MATLAB code to making design constraints, all their contributions were equally important so I would like to take the time to list everyone who contributed to me publishing this thesis at various stages of this project.

Student Colleagues

Andrew Steen……The Ohio State University

Dennis Scott……The Ohio State University

Taylor Watson……Auburn University

Josh Latimer……...The Ohio State University

Justin Clark……The Ohio State University

Experienced Engineers from NASA Johnson Space Center

Luke McNamara……...EG-5, Trajectory Design Branch

Eric Hurlbert……..EP-4, Space Propulsion Branch

John Scott……..EP Division Chief Technologist

Ron Sostaric…… EG-5, Trajectory Design Branch

Ohio State University Faculty

Dr. Ali Jhemi……Associate Professor, Specialization in Controls

Dr. Prasad Mokashki……..…..Professor, Specialization in Mechanics and Materials

Table of Contents

Chapter 1 - Introduction 1
1.1 Scoping Out Lunar Soil for Resources 1
1.1.1 The Need for a Lunar Hopper 2
1.2 Literature Review 5
1.2.1 Lunar Science 5
1.2.2 How Lunar Soil and Materials can enable Sustainability 5
1.2.3 Scientific Instrumentation 7
1.2.4 Brief Overview of Nuclear Thermal Propulsion 7
1.2.5 NTP Engines Analyzed for Integration 10
Chapter 2 - Methodology 13
2.1 Constraints and Assumptions 13
2.2 Program Description 15
2.2.1 Initialization of Variables 15
2.2.2 Setting Up Restart Altitude 15
2.2.3 Setting Up Mass and Recording Time 16
2.2.4 Ascent 16
2.2.5 Coast 19
2.2.6 Descent 20
2.3 Data Acquisition 23
2.4 Trajectory Plotting 24
Chapter 3 - Results 25
3.1 General Trends 25
3.2 Critically Limited Performance 26
3.3 SNRE and Peewee Performance 31
3.4 Selecting the Design 32
3.5 Maximizing Performance 34
Chapter 4 - Design 37
4.1 Initial Sizing of the Vehicle 37
4.2 Design Layout 39
4.3 Structures 42
4.3.1 Main Chassis/Scientific Bay 44
4.3.2 Landing Gear 46

4.4 Engine 46
4.5 Control 48
4.5.1 Computer, Avionics and GNC 49
4.6 Communications 50
4.7 Power 50
4.8 Thermal Systems 52
4.9 Concerns and Considerations 52
4.9.1 Zero-Boil-Off 53
4.9.2 The Restart Problem 53
4.9.3 Radiation impact on Lunar Environment 54
Chapter 5 - Final Vehicle Performance 55
Chapter 6 - Conclusion 57
Appendix A 58

List of Figures

Figure 1: Landing Site of Apollo 11, overlaid with the background of a Soccer Field ("Apollo Traverses on Earth, n.d.) 2
Figure 2: Composition of Typical Mare Basalts sampled from rocks returned from the Apollo Missions (Heiken, G. et all, 1991) 6
Figure 3: Equation for Effective Velocity (Dave, 2015)....8
Figure 4: Diagram Illustrating a sample NTP Engine in Detail (Belair et al ,2013) 9
Figure 5: Fuel Element (left) and Tie-Tube (right) (Belair et al ,2013)....10
Figure 6: Peewee Engine on a Test Stand ("Project RHO: Engine List 2", n.d.)....11
Figure 7: Graphics of the Criticality-Limited NTP Engine and SNRE Engine ("Project RHO: Engine List 2", n.d.) 11
Figure 8: Free Body Diagram and Velocity Vectors of Vehicle During Ascent....17
Figure 9: Illustration of Program verifying if the Vehicle is hitting the Target Distance at a Moment "t"....18
Figure 10: Illustration of Vehicle Traveling During Coast Segment....19
Figure 11: FBD of Vehicle during Phase I of Powered Descent....21
Figure 12: Vehicle during Phase II and III of Powered Descent....22
Figure 13: Initial Trajectory Plots....35
Figure 14: Refined Trajectory Plots....36
Figure 15: Ballooned Drawing of Hopper....39
Figure 16: Vertical views of the hopper looking down on the Spacecraft....39
Figure 17: Drawing of Lander with units (mm) 40
Figure 18: 3D-Graphic Highlight the Location of the Center of Gravity 40
Figure 19: Schematic of Centaur Fuel Tank (NASA TM X-1844, 1970)....43
Figure 20: Schematic of a SNRE used for the CAD model (Project RHO: Engine List 2, n.d.) ..47
Figure 21: Full Dimensioned Drawing of LH2 Fuel Tank (mm) 58
Figure 22: Full Dimensioned Drawing of Octagonal Base (mm)....58
Figure 23: Full Dimensioned Drawing of SNRE (mm) 59
Figure 24: Vertical View of Engine Shaft (mm) 59
Figure 25: Horizontal View of Engine Shaft (mm) 60
Figure 26: Fully dimensioned schematic of Landing Leg (mm) 61
Figure 27: Fully Dimensioned Schematic of GNC and Communications "Hat" (mm) 61

List of Tables

Table 1: Potential NTP Mission Matrix for the 3 NTP Engines Analyzed (Borowski & McCurdy, 2017) 12
Table 2: Performance Parameters for Study (Project RHO: Engine List 2, nd) 14
Table 3: An Example Set of Performance Data for the Critically Limited Engine, MR=2.625, 5 km trajectory 27
Table 4: Example Performance Data for the SNRE Engine, MR=3.375, 5 km trajectory 29
Table 5: Example Performance Data for the Peewee Engine,MR=4.125, 5 km trajectory 30
Table 6: Highlighted MR's and Engine Combinations for the SNRE and Peewee Class Engines 31
Table 7: Maximum Number of Hops for SNRE, MR=3.375, Dry Mass: 3500 kg 36
Table 8: Maximum Number of Hops for SNRE, MR=2.625, Dry Mass: 4500 kg 36
Table 9: All Mass Properties of Relevant Subsystems 41
Table 10: Power Requirements for Subsystems 51
Table 11: Power Consumption and Mass (Larson & Wertz, 1997, p.334) 52
Table 12: Table of Non-Refined Performance Data for a Dry Mass of 3724 and 4071 kg with a gamma1 of 45 degrees 55
Table 13: Table of Non-Refined Performance Data for a Dry Mass of 3724 and 4071 kg with a gamma1 of 60 degrees 55

Symbols for Equations

ΔV ..... Change in Velocity ("Delta-V")

g_0 ..... Uniform Gravity Constant on Earth

Isp ..... Specific Impulse

M_f ..... Final Mass

M_i ..... Initial Mass

$\dot{m}$ ..... Mass Flow Rate

a_{thrust} ..... Net Acceleration

V_y ..... Y Velocity Component

V_x ..... X Velocity Component

$h_{@instant}$ ..... The Altitude at an Instance "t"

$d@instant$ ..... The Horizontal Travel Distance at an Instance "t"

g ..... Uniform Gravitational Constant on the Moon

Δt ..... Increment of Time Changed

a_x ..... Acceleration in X Direction

a_y ..... Acceleration in Y Direction

γ_1 ..... Flight Path Angle for Ascent

γ_2 ..... Flight Path Angle for Descent

σ_x ..... Stress

$\sigma_{ulimate-yield}$ ..... Ultimate Yield Stress

$\sigma_{fatigue}$ ..... Fatigue Stress

I_{axis} ..... Moment of Inertia Acting on an Axis

τ_{max} ..... Maximum Torque

α_{axis} ..... Angular Acceleration

$\Delta\theta$ ..... Change in Angle

θ_0 ..... Initial Angle

ω_0 ..... Initial Angular Velocity

Chapter 1 - Introduction

1.1 Scoping Out Lunar Soil for Resources

Recently, there has been a renewed interest in returning a human presence to the Moon, particularly a permanent one. In March 2019, President Donald J. Trump mandated that NASA return astronauts to the Moon within 5-year time frame. Commercial companies such as SpaceX and Blue Origin have also shown an interest in returning astronauts to the moon and eventually developing permanent habitations. With this renewed 21st century interest in the moon, one of the largest technical challenges is not just “How can we get there?”, it is also: “Where do we go?”. If humans are to eventually settle the moon permanently and sustainably, one important requirement is the capability to select landing sites based on soil content, measured from actual physical samples.

Most of the Moon remains unexplored. From all six Apollo Landings, approximately 382 kg (842 lbs.) of soil and samples were returned for further analysis and testing on Earth ("Lunar Rocks and Soils from Apollo Missions," 2016). In order to characterize large portions of the lunar surface and subsequently influence landing site selection based on available resources, significantly more soil samples would need to be collected.

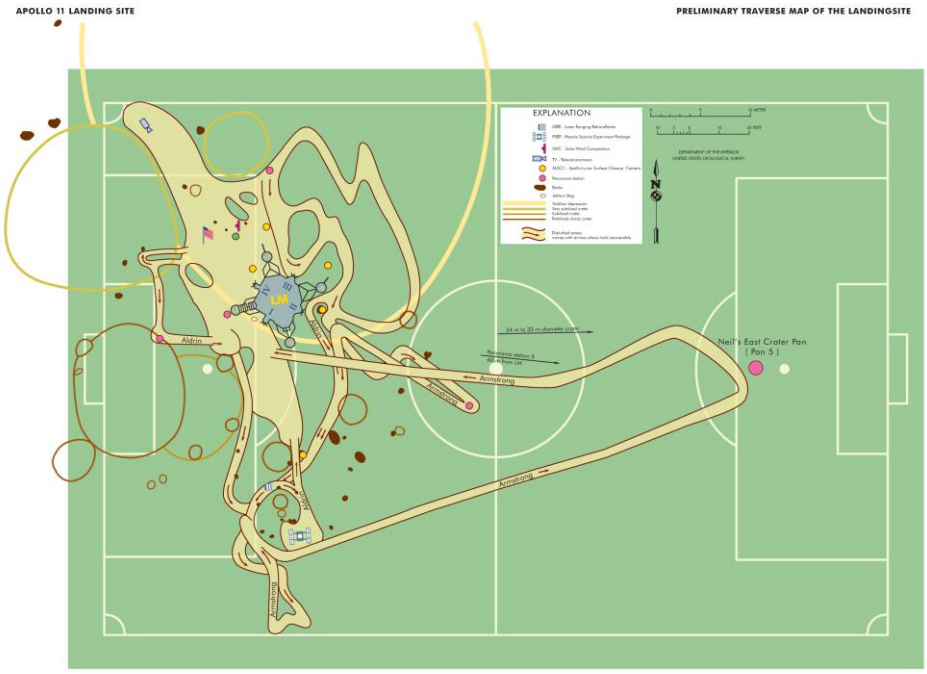

Figure 1: Landing Site of Apollo 11, overlaid with the background of a Soccer Field ("Apollo Traverses on Earth, n.d.)

1.1.1 The Need for a Lunar Hopper

The figure above (Figure 1) shows a representation of the superimposed *Apollo 11* landing site onto the background of a soccer field. This figure illustrates just how little surface area of the Moon that has been physically explored. The Moon and the continent of Africa share roughly the same surface area for comparison sake, and it is apparent that a mere six manned landing sites and number of unmanned probes/landers in single-isolated locations do not present the full picture of what the Moon can offer.

In 2009, (37 years after the last pair of humans visited the surface) the scientific community's understanding of the Moon changed dramatically when LCROSS, an impactor probe, hit Shackleton Crater on the lunar South Pole (Spudis, 2013). The Lunar Reconnaissance Orbiter (LRO) verified via hyperspectral analysis that large deposits of ice exist on the bottom of Shackleton Crater (Spudis, 2013). This major discovery would not have been possible if the

material lying on the bottom of the crater wasn't analyzed in further detail. It is clear that major groundbreaking discoveries relating to the Moon and its resources can happen if the investment is made.

If any sort of entity wishes to permanently settle the moon, more data must be collected to support the selection of suitable landing sites. Shackleton Crater on the lunar south pole has been highlighted as a prime target for manned missions or settlements due to its substantial sources of water, sunlight and permanent shadow. Shackleton Crater is only one specific location and does not give the full picture of what the Moon has to offer. Satellites (such as the LRO) have mapped the moon in detail using spatial, spectral or temporal scanners and instruments but fail to display the level of detail needed to confirm if materials exist in harvesting resources for permanent settlement. Materials such as aluminum, titanium, iron would be important for sustainable human presence to develop infrastructure to manufacture structural components need for habitats or spacecraft. In-Situ Resource Utilization (ISRU) is needed to validate and refine the measurements gathered from satellites in lunar orbit. Information and knowledge can be refined further with data gathered from lunar material and physical samples that can be observed.

It would be expensive and logistically implausible to send "flag and footprint" style missions to enough locations on the moon to select an ideal location for permanent settlement. One alternative to this is the use of a smaller number of unmanned vehicles capable of covering more area over a longer period of time.

Roving vehicles have been engineered and utilized in the past for both Lunar and Martian exploration. The fundamental limitation of rovers is energy. Rovers are battery driven, making them useful assets for short range exploration only. Furthermore, rovers are constrained to certain types of terrain. If obstacles such as mountains or steep craters exist in the way of a

target destination for sampling, a rover would be forced to spend a long amount of extra time going around a circular route or risk being toppled over as it travels across steep terrain.

This paper will discuss an alternative to roving vehicles: a lunar hopper. A lunar hopper is a vehicle that can take off and land repeatedly for the purpose of taking soil samples from multiple locations on the lunar surface. Traditionally, lunar landing vehicles (such as Surveyor, the Apollo Lunar Module, Beresheet, etc.) have utilized hypergolic chemical rocket engines, which are limited in their efficiency (specific impulse/Isp) and require very dense propellants. A more efficient alternative is an electric ion propulsion system, which uses electric energy to heat an inert gas propellant such as neon or xenon into a plasma. While this system is very efficient, it typically produces thrust on the order of micronewtons (Jones, 2017). Thus, it is not feasible for use in a lunar hopper vehicle due to the thrust to weight ratio (TWR) being far lower than one. Another high-efficiency alternative is a Nuclear Thermal Propulsion (NTP) system, which is offers double/triple the specific impulse and comparable thrust to conventional liquid rocket engines. While it is infeasible for a launch vehicle on Earth to use an NTP engine (due the smaller amount of thrust, atmospheric drag weakening performance and concerns with radioactive pollution), on the Moon there is only one-sixth gravity and it is nearly a perfect vacuum. Thus, it represents a satisfactory compromise between the extremes of traditional liquid rocket engines (high thrust/low efficiency) and electric ion thrusters for this specific application (really low thrust/ really high efficiency).

1.2 Literature Review

1.2.1 Lunar Science

The hopper is primarily designed to help aid scientists and policy to discover and find soil contents that can aid in producing structures and consumables for a permanent human settlement.

While the Apollo missions had a good diversity of scientific experiments to test on the lunar surface, the scientific mission for the hopper is to look at the contents of the soil and determine if the findings would warrant a manned visit or permanent settlement should take place in the same location.

1.2.2 How Lunar Soil and Materials can enable Sustainability

Below is a table of sample elements and compounds that were found in trace rock samples during the Apollo Missions. It is important to keep in mind the goals were to investigate locations that could help explain the geological history of the Moon with sites using near the equator which were chosen due to the free return trajectories the Apollo Program used and Delta-V limits (Heiken, Vaniman & French, 1991). The emphasis for this project is to find landing sites that would help enable sustainability for a permanent human presence.

Table IV. – Composition of Mare Basalts

	12002	12005	70017	74220
SiO_2	43.56	41.56	38.54	38.57
TiO_2	2.6	2.72	12.99	8.81
Al_2O_3	7.87	5.3	8.65	6.32
Cr_2O_3	0.96	0.75	0.5	0.75
FeO	21.66	22.27	18.25	22.04
MnO	0.28	0.3	0.25	0.3
MgO	14.88	10.07	9.98	14.44
CaO	8.26	6.31	10.28	7.68
K_2O	0.05	0.04	0.05	0.09
Na_2O	0.23	0.16	0.39	0.36
P_2O_5	0.11	0.04	0.05	
S	0.06	0.04	0.16	
Total	100.43	99.46	100.59	99.06

Figure 2: Composition of Typical Mare Basalts sampled from rocks returned from the Apollo Missions (Heiken, G. et all, 1991)

ISRU is the art of processing raw materials from celestial destinations and converting them to useable materials for manned or unmanned space missions. Chemical reactions can allow for the ability to mine, separate compounds and harvest useful minerals and alloys. Many of the compounds can be converted to oxygen which can serve either as a consumable for astronauts to breathe or it could be converted to oxidizer propellant. Even if the percentages of certain compounds are low, one must take in consideration the absolute abundance of minerals are on the surface of the moon. Many NASA centers have made investments into researching these methods and they could be integrated into future space missions with some key tests having been demonstrated for application of lunar missions. (Zacny, 2012).

Helium-3 is another reason why people are targeting lunar resources because it could provide waste-free nuclear power. Unlike the Earth, the Moon is thought to have significant deposits of Helium-3 as a result of solar winds hitting the surface due to no substantial atmosphere shielding it. These are one of the reasons why the Chinese Space Program has taken a key interest in lunar exploration (Barnett, 2016).

1.2.3 Scientific Instrumentation

In recent years successful unmanned missions to the surface of Mars have been enabled by the use of mass spectrometry. The Mars Curiosity Rover has many instruments such as alpha particle x-ray scanners, chemical cameras and mineralogy scanners, sample analysis and radiation assessment detectors (“NASA Curiosity Rover Instruments”, n.d.). These lightweight instruments have helped scientists analyze and better understand the Martian environment. Similar instruments can be integrated on a vehicle that can tell us more about the lunar surface. Likely a hopper would need to be able to scoop up soil samples on the surface, attain samples from beneath the surface using a drill and have sensors to scan the nearby surface and identify the materials the soil contains. Small rovers can also be stored and deployed once a hopper touches down so a region can be explored more in depth within a certain radius. A robotic arm might be useful as well in order to ensure the vehicle can perform a multitude of tasks with regards to being able to collect data and complete experiments.

1.2.4 Brief Overview of Nuclear Thermal Propulsion

NTP has been tested extensively in the 1950s-1970s through Project Rover: a joint research venture between Los Alamos Laboratory and NASA to develop NTP engines that were envisioned to aid in human missions to Mars. When the Apollo Program was cut short and the focus of human space exploration shifted completely to the Space Shuttle Program, Project Rover was subsequently canceled. While the NTP test articles were never flown, the data collected from the program has built the backbone of engineering knowledgebase behind NTP systems.

In 2019, funding has been allocated to Marshall Space Flight Center and its contractor BWXT to build and design next generation concepts based on Low-Enriched (non-weapon grade) Uranium (Mohon, 2017).

NTP engines attain such a high efficiency because of effective exit velocity. Specific impulse is equal to the exit velocity divided by 9.81 m/s^2 (Earth’s gravitational acceleration constant).

Unlike a conventional rocket, there is no combustion from a chemical reaction occurring. Thrust is produced by simply heating liquid hydrogen (LH2) to a hot gas and expanding it through a rocket nozzle.

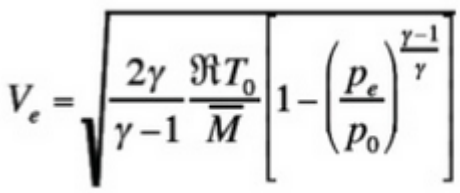

$$V_e = \sqrt{\frac{2\gamma}{\gamma - 1}\frac{\Re T_0}{\overline{M}}\left[1 - \left(\frac{p_e}{p_0}\right)^{\frac{\gamma-1}{\gamma}}\right]}$$

Figure 3: Equation for Effective Velocity (Dave, 2015)

Looking at the equation in Figure 3: the variable M represents the molecular mass of the propellant, gamma represents the ratio of specific heats, R is the universal constant, T_0 is the temperature in the thrust chamber, P_0 is the pressure in the Thrust chamber and P_e in exit pressure out the end of the nozzle. Hydrogen is the second lightest element in the periodic table having a molecular mass of only 2.08 g/mol (the most efficient [operational] liquid chemical propulsion system LOX/LH2 has a molecular mass of 13.2 g/mol.) The molecular mass of the propellant is inside the radicand and is being divided from the product of the gas constant and chamber temperature. Decreasing the molecular mass yields a higher product inside the radicand. Thus, referencing the equation it is apparent that the lighter the propellant, the higher the effective velocity, and thus the higher the specific impulse. A nuclear reactor provides the thermal power needed for high temperatures in the thrust chamber (2500-3000 K) by using the process of fission (Belair,Sarimento & Lavelle,2013).

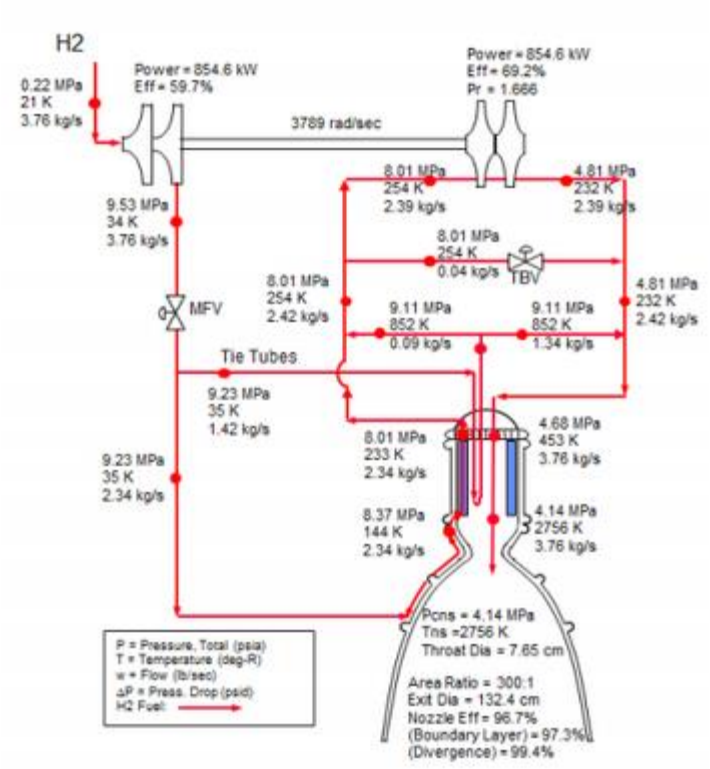

Figure 4: Diagram Illustrating a sample NTP Engine in Detail (Belair et al ,2013)

The graphic above shows a schematic of an NTP engine with the LH2 as the working fluid driven by a turbopump. In this specific example an expander cycle engine is being utilized and hot-gas from the thrust chamber drives the turbine that provides power to the compressor goes and comes back to be expelled out the nozzle. Fuel goes from the tank, through the turbopump and employs “regenerative cooling” through the channel-walls of the nozzle before entering the core reactor. In an expander cycle engine, all the propellant is used to produce thrust.

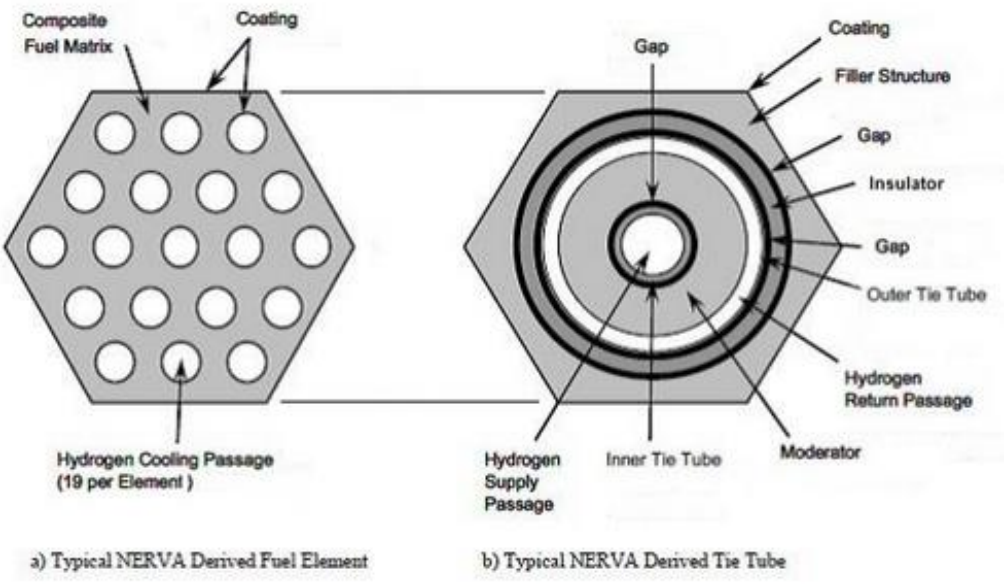

Figure 5: Fuel Element (left) and Tie-Tube (right) (Belair et al ,2013)

Inside the core of the reactor are long rods called fuel elements and tie-tubes" that typically have hexagonal cross-sections. Inside the fuel elements are channels through which the hydrogen passes and is heated to a hot gas that is expanded out of the nozzle. Tie-tubes support the reactor structurally, collect thermal energy to run the turbopumps and help reduce the structural loading on fuel elements (Belair et al, 2013).

1.2.5 NTP Engines Analyzed for Integration

Dr. Stanley Borowski of NASA Glenn Research Center in Cleveland, OH is one of the world-renowned experts regarding NTP technology. (Reference)He and his team have researched many NTP systems for a multitude of applications both analyzing hardware from Project Rover/NERVA and theorizing more modern systems. Some of the concepts included integrating NTP on unmanned and manned landers for lunar and Martian Exploration. From *Project Rover*, several engines were designed, built and tested. For this study, a custom NTP engine does not need to be designed from scratch, rather previous hardware already built/theorized is analyzed for potential integration.

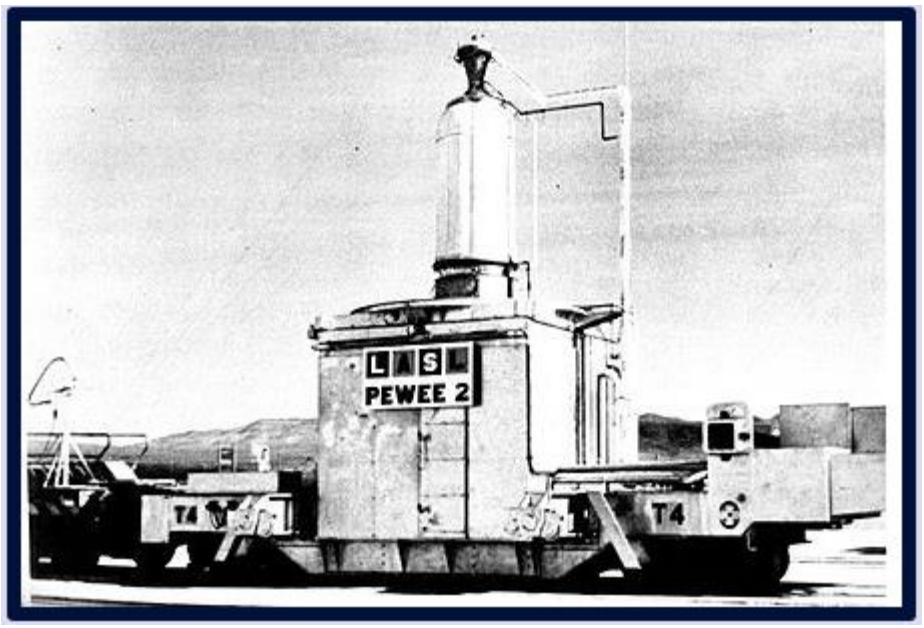

Figure 6: Peewee Engine on a Test Stand ("Project RHO: Engine List 2", n.d.)

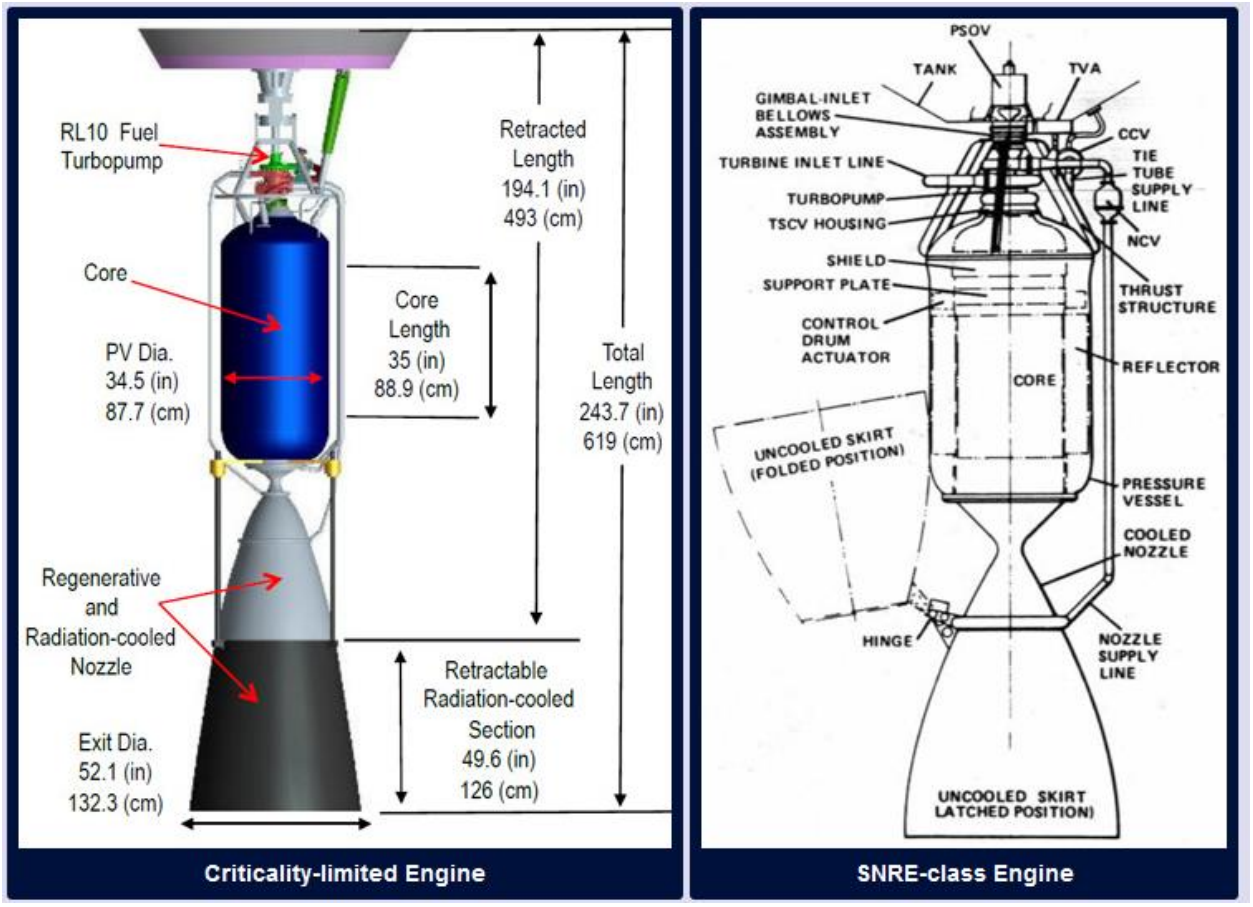

Figure 7: Graphics of the Criticality-Limited NTP Engine and SNRE Engine ("Project RHO: Engine List 2", n.d.)

Requirements / Missions	Engine Thrust (klb_f)	T/W_{eng}	T_{cx} (°K)	I_{sp} (s)	No. Engines	Fuel Loading (gU/cm^3)	U-235 Mass (kg)	Longest Single burn (min)	Total burn duration (min)	No. burns
Robotic Science	7.4	~1.9	2736	894	1	0.6	27.5	~22	~29.5	2
Lunar Cargo	16.7	~3.1	2726	900	3	0.6	60	~21.4	~49.2	5
Lunar Piloted	16.7	~3.1	2726	900	3	0.6	60	~20.9	~55	5
NEA - *Apophis* Piloted	25	~3.5	2790 - 2940	906-940	3	0.25	36.8	~25 - 37.2	~43.8 - ~77.3	4-5
Mars Cargo	25	~3.5	2790 - 2940	906-940	3	0.25	36.8	~22	~38	2
Mars Piloted	25	~3.5	2790 - 2940	906–940	3	0.25	36.8	~44.5	~79.2	4

Table 1: Potential NTP Mission Matrix for the 3 NTP Engines Analyzed (Borowski & McCurdy, 2017)

Three NTP engines stand out for their smaller size and thrust that maybe suitable for a lunar lander: Critically Limited (7.4 klbf of thrust), Small Nuclear Reactor Element (SNRE) (16.7 klbf of thrust) and the Peewee (25 klbf of thrust). All three engines are listed in the table above for their thrust output and their potential application. The Critical Limited Engine and SNRE are theorized while the Peewee Engine was based on real hardware (“Project RHO: Engine List 2”, n.d.).

The Critically-Limited is the minimum size of what an NTP engine can realistically be based on the minimum amount of fuel (Uranium in this specific case) required for fission to take place. It is only theorized for small robotic missions (Borowski & McCurdy, 2017). SNRE produces more than double the thrust of Criticality-Limited and can complete a wider variety of missions. The Peewee engine was the “smallest” from *Project Rover* that was built and tested but it is large enough to be a contender for a spacecraft that can complete a Trans-Mars Injection if used in pairs or triplets (Borowski & McCurdy, 2017).

Chapter 2 - Methodology

This project was focused on using analytics, optimization methods and data science to figure out the what combinations produced the most optimum vehicle performance measured by the number of hops each vehicle could complete. The goal was to create trajectories and analyze them by varying certain of physical characteristics of the vehicle. The following parameters were varied: the engine, the initial mass (or dry mass), the Mass Ratio (MR) [(maximum propellant mass plus dry mass) over dry mass], the initial flight path angle relative to the surface (gamma), the altitude for restarting the engine for powered decent and the travel distance from launch to landing. With the data gathered from the study the overarching goal was to determine how to maximize the total number of hops from a theoretical point of view and then use real world constraints to create a feasible and practical design. To acquire this data, MATLAB was used as the primary programming language to create each simulated trajectory. The main program was created integrated with several functions, nested loops and conditional statements to create each phase of flight for each hopper MR.

2.1 Constraints and Assumptions

Below are the three engines and the corresponding dry-masses: 2500 kg, 3500 kg and 4500 kg respectively. These dry masses are driven by the rocket equation as a starting point to account for the corresponding size and estimated structure needed for the engine.

$$\Delta V = (g_0 Isp) In(\frac{M_i}{M_f}) \qquad (2.0)$$

Name	**Vehicle Dry Mass (kg)**	**Thrust (kN)**	**Specific Impulse (s)**	$\dot{m}$ **(kg/s)**	**Mass of Engine (kg)**
Critically Limited	2500	32	894	3.8	1770
SNRE	3500	74	900	8.4	2400
Peewee	4500	111	940	12.5	3240

Table 2: Performance Parameters for Study (Project RHO: Engine List 2, n.d.)

Once the optimum combination (MR, engine and dry mass) is selected the dry mass will serve as a starting point and the mass will be defined further with more detail by creating conceptual designs for subsystems the lander will need.

Increasing Isp yields higher amounts of ΔV, however the MR must also be considered and is in fact weighted more heavily because its relationship is logarithmic. High Isp does not guarantee optimum performance for this application and the combination of both factors will dictate final vehicle performance.

Table 2 highlights their performance criteria such as Isp, thrust, mass flow rate at maximum throttle and mass. Since the final product of this study is an actual proposed design, the range of MRs tested were from 1.5 to 9 with increments of 0.375. The upper limit was referenced off the mass ratio of the Centaur booster.

Since the hopper flies suborbital trajectories, equations of projectile motion are utilized. This allows for easier analysis than propagating extremely elongated orbits forward and backwards. For this initial study, many real-life constraints were heavily relaxed. Firstly, the lunar surface is assumed to be flat.

Secondly, the Moon's gravitational field was assumed to be uniformly one-sixth's earth's gravity. To simplify the study, an average value of 1.63 m/s^2 was used to allow the results to be comparable to one another. Analyzing the variable gravitational gradient would be an appropriate next step for detailed mission-design.

The LH2 is also assumed to be 100% useable, not considering any boil-off.

The primary focus of the study was horizontal travel distance and the number of hops successfully completed. This is because analyzing many lunar samples with healthy variety is highly desired. With this being main philosophy of the simulation, the apolune (the apex of the trajectory) is not constrained in order maximize the capability to attain samples of soil from

different regions. Using fuel to achieve an Apolune constraint would risk producing less-desirable results because the problem would be over-constrained.

For Ascent the velocity and thrust vectors are always aligned, while for Descent the thrust vector is applied in a retrograde direction. Steering losses are ignored for each simulation.

2.2 Program Description

The MATLAB Algorithm utilized has several key components for producing data: the ascent function, the coast function, the powered descent function and functions for processing data and producing plots. All units are in SI.

2.2.1 Initialization of Variables

The main research program begins with initializing the set of conditions that affect the conditions of the spacecraft. The thrust at full throttle, the Isp and gamma angles are all set as constant values.

2.2.2 Setting Up Restart Altitude

The engine, acceleration, the spacecraft mass and the restart altitude for powered decent are all interconnected. If the spacecraft starts firing the engine too soon, it will deplete fuel unnecessarily and it will either run out of fuel by the time it reaches the surface, compromising the number of hops it can complete. If it fires the engine too late, the spacecraft might not have the acceleration to reduce the velocity in time enough to land safely and it will crash into the surface. The ideal restart ratio varies based on the mass of the spacecraft, the engine and the target travel distance.

Thus, the first for loop initializes a factor called h_{ratio} which is the ratio of the restart altitude over the altitude of the apolune ranging from 0.15 to 0.99. With this feature integrated into the program, it saves time and effort finding the optimum restart altitude. Instead of finding each specific restart altitude for every trajectory and given MR it loops through all of them, and outputs which restart altitudes can land the vehicle safely on the surface automatically.

2.2.3 Setting Up Mass and Recording Time

The second for-loop of the program varies the MR from 1.5 to 9 on increments of 0.375. Here the number of hops is initialized with the value of 0 for every new MR.

Within the MR loop is a nested for-loop for program control acts, a clock counting from 0 to 36000 seconds (10 hours). The large amount of time is used to ensure that there won't be any risk of ending the program when the lander still has useable fuel on-board. Each hop starts and ends consecutively with no breaks or stay on the surface. The variable Δt, is constant and is kept at 0.25 seconds. Δt is the step-size of the counting for-loop and all velocity and distance values are calculated iteratively using it.

There is a flag variable called "s" that tells the main program when to execute each function. The value of s is set to 1,1.5 and 2 to run the ascent, coast and descent programs respectively. The flag is set to -1 if the lander crashes at any point. The flag is checked for using if and else statements.

2.2.4 Ascent

The first function (or phase of flight) is the ascent function. The function fires the engine at full throttle with the designated value of gamma1 set at 45 degrees. While the engine fires, the new mass and acceleration are calculated using $\dot{m}$. The two forces acting on the spacecraft while the engine is firing are gravity and thrust. If the vehicle is unable to produce a positive acceleration in the y-direction, the velocity and distance values are set to 0 and the vehicle keeps burning fuel until the TWR is large enough to get the vehicle off the ground.

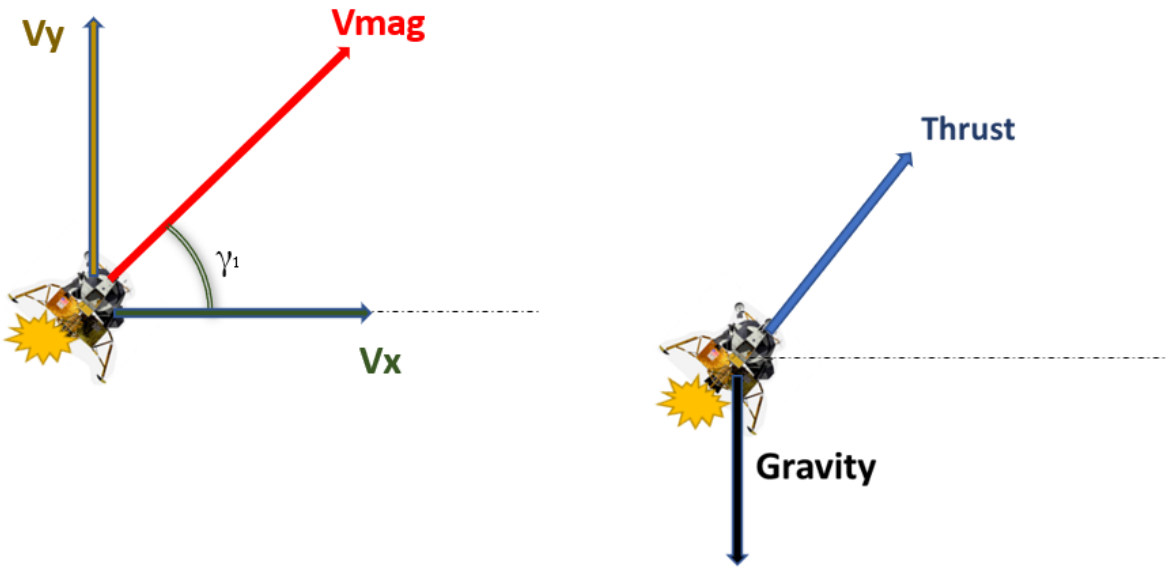

Figure 8: Free Body Diagram and Velocity Vectors of Vehicle During Ascent

Engine On:

$$M_f = M_i - \dot{m} * \Delta t \quad (2.1)$$

$$a_{thrust} = \frac{T}{M_f} \quad (2.2)$$

$$a_x = \frac{T}{M_f}\cos(\gamma_1) \quad (2.3)$$

$$a_y = \frac{T}{M_f}\sin(\gamma_1) - \mathrm{g} \quad (2.4)$$

$$V_y = a_y \Delta t + V_{y\_initial} \quad (2.5)$$

$$V_x = a_x \Delta t + V_{x\_initial} \quad (2.6)$$

$$h_{@instant} = \frac{1}{2} a_y \Delta t^2 + V_{y\_initial} \Delta t + h_{initial} \quad (2.7)$$

$$d_{@instant} = \frac{1}{2} a_x \Delta t^2 + V_{x\_initial} \Delta t + d_{initial} \quad (2.8)$$

Verifying if target requirement is met

$$M_f = constant \quad (2.9)$$

$$a_x = 0 \quad (2.9)$$

$$a_y = -\mathrm{g} \quad (2.10)$$

$$\Delta t_{@ascent\ shutdown-apolune} = \frac{V_y}{g} \quad (2.11)$$

$$V_{y@apolune} = 0 \quad (2.12)$$

$$\Delta t_{h_{apolune}-impact} = \sqrt{\frac{2*h_{apolune}}{g}} \quad (2.13)$$

$$\Delta t_{impact} = \Delta t_{@instant-ap} + \Delta t_{h_{apolune}-impact} \quad (2.14)$$

$$\Delta x_{impact=} V_x * \Delta t_{impact} + \Delta x_{@ascent\ shutdown-launchsite} \quad (2.15)$$

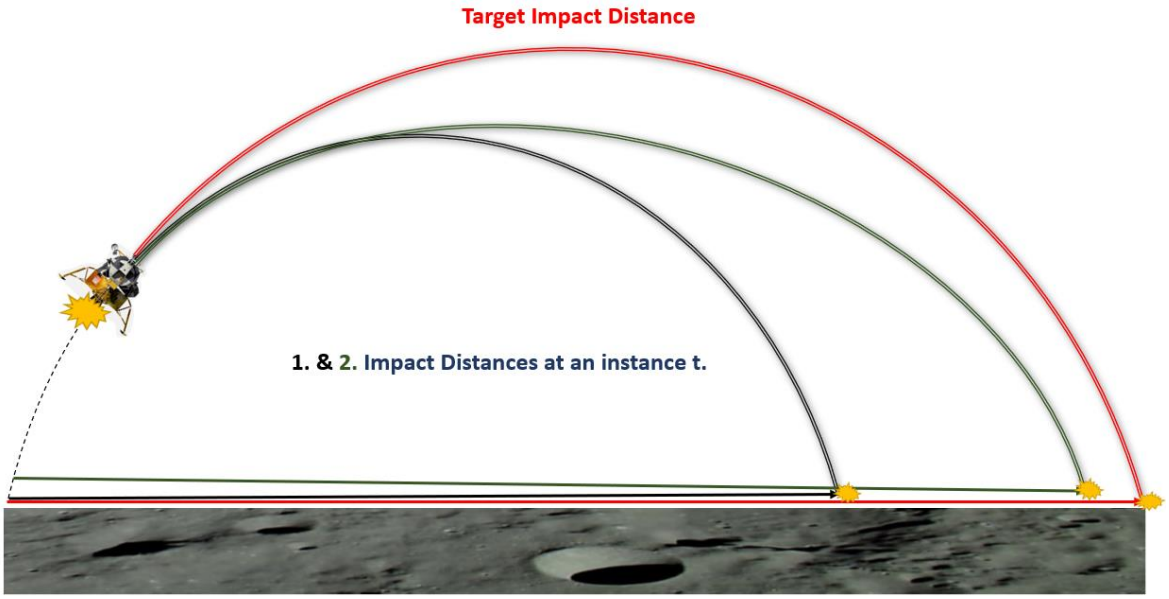

Figure 9: Illustration of Program verifying if the Vehicle is hitting the Target Distance at a Moment "t"

Using the following kinematic equations, the values for acceleration, velocity and distance are calculated. The origin is always set from the point of take-off. T

As the function executes, it is checking if the vehicle would hit the target travel distance (5 km, 10 km, 25 km) if the engine shut down at that instant (referencing a set of equations with only gravity acting on the lander.) Once it verifies that the spacecraft has hit the horizontal target the engine shuts off, s is set to 1.5 and the relevant values (time, altitude, horizontal distance) are recorded.

The ascent program also checks to verify the lander still has propellant mass on-board. If not, the vehicle is marked as having crashed and then moves to the next MR.

2.2.5 Coast

$$M_f = const \quad (2.16)$$

$$a_x = 0 \quad (2.17)$$

$$a_y = -\mathrm{g} \quad (2.18)$$

$$V_y = a_y \Delta t + V_{y\_initial} \quad (2.19)$$

$$V_x = const \quad (2.20)$$

$$h_{@instant} = \frac{1}{2} a_y \Delta t^2 + V_{y\_initial} \Delta t + h_{initial} \quad (2.21)$$

$$d_{@instant} = V_x \Delta t + d_{initial} \quad (2.22)$$

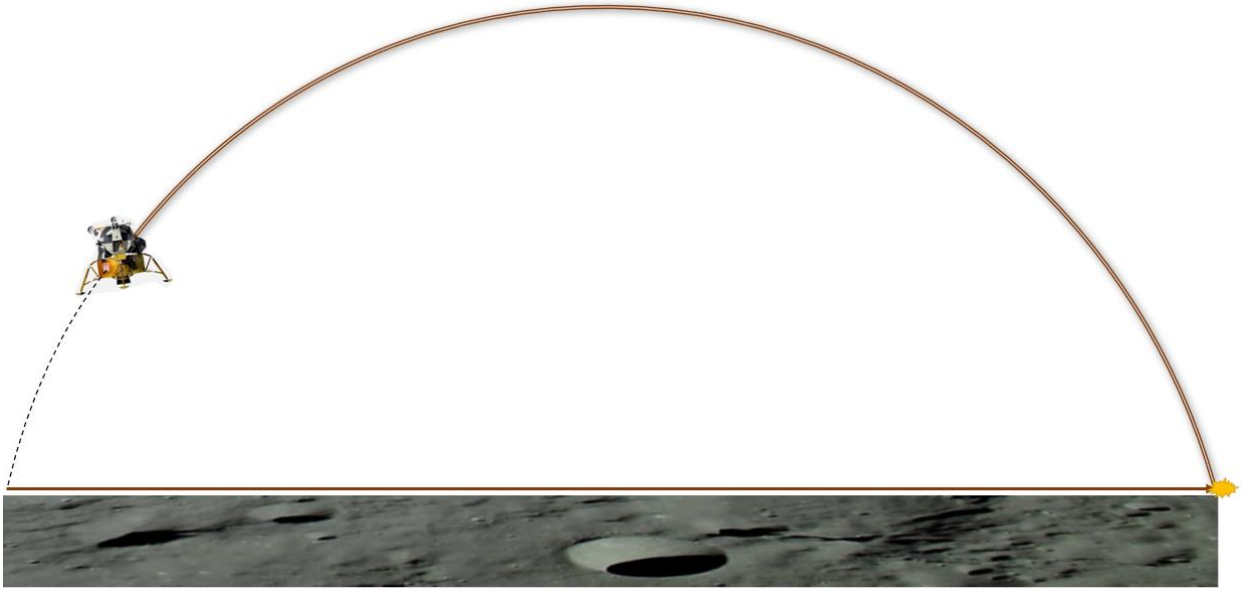

Figure 10: Illustration of Vehicle Traveling During Coast Segment

The coast function takes in the value of h_{ratio} and sets the restart altitude based on what the value of Apolune for that corresponding hop. The coast function then calculates various parameters such as time until reignition, the y-velocity at the point of restart and γ_2. The coast calculation assumes the engine is off and only the gravity of the Moon is acting on the spacecraft. The program continues to calculate and check the new velocity and altitude after the

coast function is executed. The descent program starts when the vehicle falls below the restart altitude.

2.2.6 Descent

The descent function focuses on the most dynamic portion of flight: powered descent. Like the Ascent function it also utilizes a while loop. The function initiates when the altitude of the spacecraft falls below the calculated altitude for restart. The spacecraft is pointed in a retrograde direction from the velocity vector and the flight path angle (gamma_2) is recalculated as Vx and Vy change to ensure the spacecraft is pointing in the right direction. The function is divided into 3 distinct phases. During powered descent, the program discounts any possible transient propellant losses during ignition or shut-down.

The first phase focuses on reducing the value of Vx down to 0 m/s, thus causing the spacecraft to descend vertically. During this time the spacecraft is at full throttle.

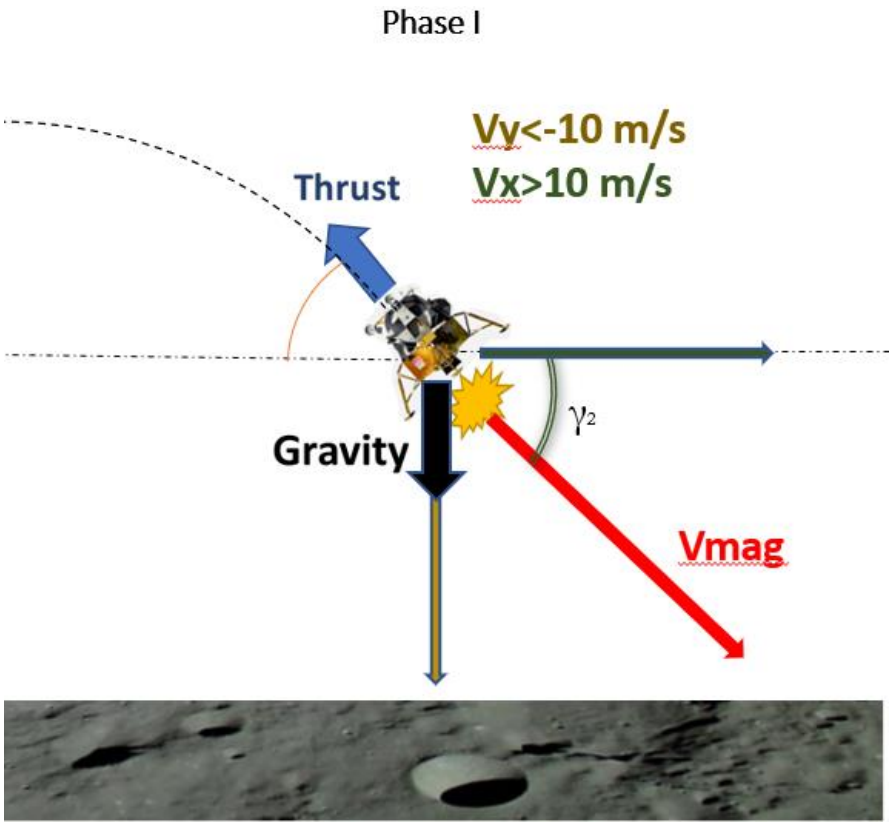

Figure 11: FBD of Vehicle during Phase I of Powered Descent

Once Vx is reduced to a value close to 0 m/s, the program sets Vx to 0 m/s manually. The Phase II is to slow down y-component of the velocity to -2 m/s. The engine is still firing at full throttle while this is occurring.

Phase I

$$M_f = M_i - \dot{m} * \Delta t \quad (2.23)$$

$$a_{thrust} = \frac{T}{M_f} \quad (2.24)$$

$$a_x = \frac{T}{M_f}\cos(\gamma_2 + 180^\circ) \quad (2.25)$$

$$a_y = \frac{T}{M_f}\sin(\gamma_2 + 180^\circ) - \mathrm{g} \quad (2.26)$$

$$V_y = a_y \Delta t + V_{y\_initial} \quad (2.27)$$

$$V_x = a_x \Delta t + V_{x\_initial} \quad (2.26)$$

$$h_{@instant} = \frac{1}{2} a_y \Delta t^2 + V_{y\_initial} \Delta t + h_{initial} \quad (2.28)$$

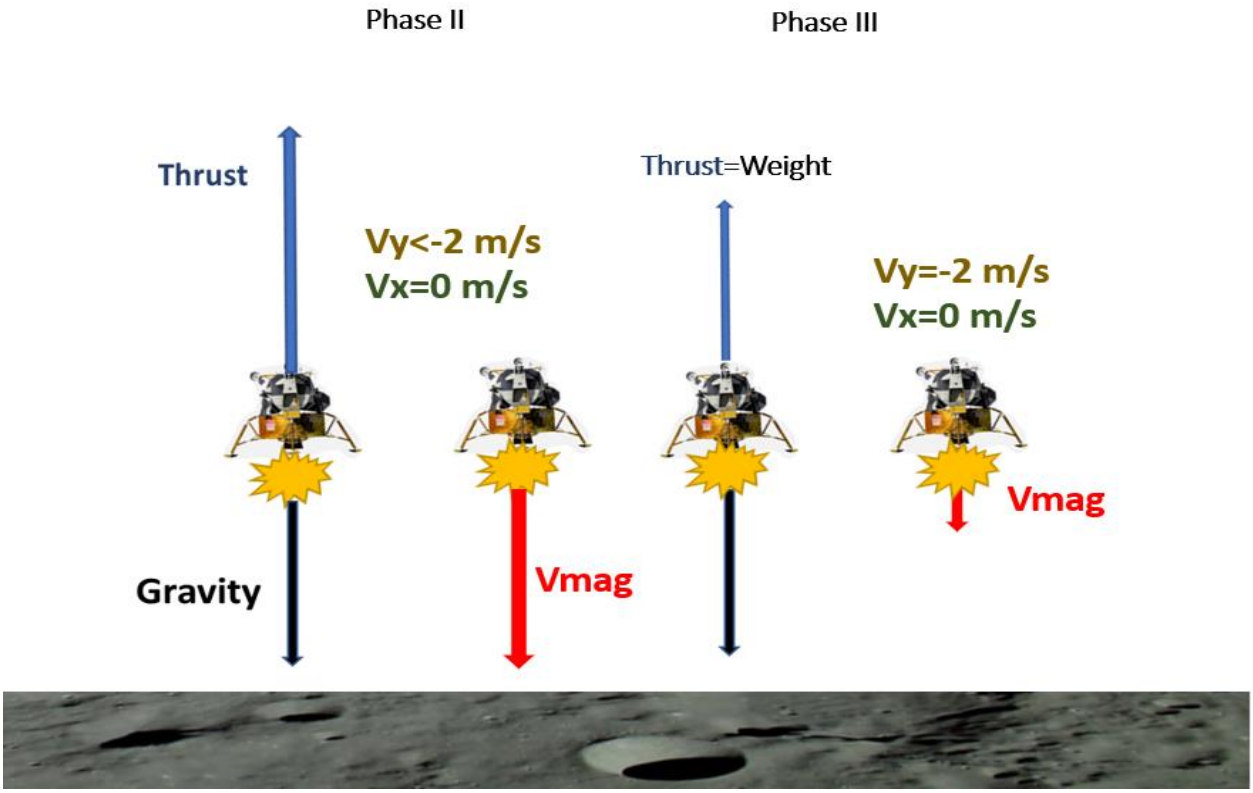

Figure 12: Vehicle during Phase II and III of Powered Descent

Phase II

$$M_f = M_i - \dot{m} * \Delta t \quad (2.29)$$

$$a_{thrust} = \frac{T}{M_f} \quad (2.30)$$

$$a_x = 0 \quad (2.31)$$

$$a_y = \frac{T}{M_f} - \mathrm{g} \quad (2.32)$$

$$V_y = a_y \Delta t + V_{y\_initial} \quad (2.33)$$

$$h_{@instant} = \frac{1}{2} a_y \Delta t^2 + V_{y\_initial} \Delta t + h_{initial} \quad (2.34)$$

$$V_x = 0\ m/s \quad (2.35)$$

Phase III

$$T = m_{dot\_LOW} * V_e \quad (2.36)$$

$$V_e = g_0 * Isp \quad (2.37)$$

$$T = W \quad (2.38)$$

$$m_{dot\_LOW\_throttle} = \frac{W}{g_0 * Isp * lossfactor} \quad (2.39)$$

$$M_f = M_i - m_{dot\_LOW\_throttle} * \Delta t \quad (2.40)$$

$$a_y = 0 \quad (2.41)$$

$$h_{@instant} = V_y \Delta t + h_{initial} \quad (2.42)$$

The final phase is the pre-touch down phase. Here Vx and Vy are treated as constant as the vehicle descends to the surface at a constant 2 meters per second. While in all previous portions of the program have fired the engine at full throttle, here the spacecraft has a net acceleration of 0. Thus, TWR is set equal to 1. A new mass flow rate is calculated by setting the thrust equal to the weight of the spacecraft and dividing by the exhaust velocity. Because there is greater entropy loss at lower throttle settings, a new exhaust velocity is calculated by refencing the Isp and an average percentage loss (Sutton & Biblarz, 2017, pg. 304). Once the altitude of the spacecraft falls below 0 meters, the engine shuts off, the number of completed hops and relevant information relating to horizontal distance, time and mass are recorded. Like ascent, the descent function checks to ensure the vehicle mass is greater than the dry mass (meaning useable propellant is still on-board) and marks the vehicle as having crashed if that is not the case. It also checks to ensure the spacecraft lands within safe velocities (Vy < 5 m/s and Vx<0 m/s) otherwise it marks it as crashed as well.

2.3 Data Acquisition

As each MR is tested, a separate function writes stored data to a function and saves as an excel spreadsheet. Every time the spacecraft lands or crashes a new row of data is written in the spreadsheet containing data relating to current mass on-board, the initial mass, the restart

altitude, the final distance away from the launch site and the total horizontal distance the vehicle has traveled.

2.4 Trajectory Plotting

A flag is set in the initial part of the program if the user desires trajectory plots. Arrays of altitude and distance values relative to the launch-site are stored and the user can have all the trajectories plotted on the same graph for a given MR. This feature can help ensure that the program was able to successfully calculate all the parameters related to the flight mechanics for each suborbital trajectory the lander is able to execute for its given MR.

Chapter 3 - Results

Over 10,000 sets of data were collected from the 3 lander concepts, potential MRs and restart altitudes set. To summarize the findings the best performance for each combination is highlighted.

3.1 General Trends

For all 3 of the conceptual landers, the best performance was found for from MR's ranging from 2.625-4.875. This highlights the complicated relationship of having too little and too much propellant on-board. If a lander has a higher MR, and thus a large amount of propellant in theory it does yield a large amount of ΔV. However, in the case of creating a hopper ΔV is only one measure of performance. The vehicle still produces the same amount of thrust which affects overall acceleration and the ability to safely land the vehicle on the surface. In order to safely slow down the vehicle, a lander with a higher MR must begin powered decent at a higher altitude which expends more fuel. A higher MR doesn't yield the most optimum results based on Newton's First law of Motion. The more mass the vehicle has, the more acceleration is needed for ascent and descent, the longer the engine must produce thrust to meet the trajectory requirements and the more fuel is spent. Likewise, the philosophy of minimizing mass shouldn't be the overarching focus as it does take propellant to complete hops. Thus, the most optimum conditions appear in the middle of the lower and higher extremes of the spectrum.

3.2 Critically-Limited Performance

MR	Mi	Mf	Apogee (m)	Restart Altitude(m)	Number of completed hops	Total horizontal distance traveled in m	h_ratio
2.625	6562.5	6408.312	906.7074	489.622	1	4917.013	0.54
2.625	6562.5	6248.348	923.6492	498.7706	2	9852.413	0.54
2.625	6562.5	6079.548	942.9193	509.1764	3	14810.09	0.54
2.625	6562.5	5905.372	940.9854	508.1321	4	19679.03	0.54
2.625	6562.5	5717.061	965.604	521.4261	5	24579.42	0.54
2.625	6562.5	5526.24	969.5952	523.5814	6	29421.98	0.54
2.625	6562.5	5327.968	972.9316	525.3831	7	34186.7	0.54
2.625	6562.5	5122.503	1008.433	544.5536	8	39040.46	0.54
2.625	6562.5	4913.36	1016.72	549.0285	9	43844.79	0.54
2.625	6562.5	4701.42	1025.148	553.5798	10	48600.55	0.54
2.625	6562.5	4494.229	1033.239	557.949	11	53326.77	0.54
2.625	6562.5	4284.771	1036.628	559.7791	12	57978.18	0.54
2.625	6562.5	4072.865	1080.306	583.3653	13	62750.2	0.54
2.625	6562.5	3865.93	1084.04	585.3815	14	67467.08	0.54
2.625	6562.5	3664.128	1081.717	584.127	15	72100.75	0.54
2.625	6562.5	3459.534	1123.191	606.5233	16	76831.94	0.54
2.625	6562.5	3261.287	1114.91	602.0516	17	81452.31	0.54

2.625	6562.5	3067.028	1156.092	624.2899	18	86187.65	0.54
2.625	6562.5	2884.357	1133.191	611.923	19	90770.31	0.54
2.625	6562.5	2704.958	1161.548	627.2357	20	95409.38	0.54
2.625	6562.5	2528.083	1188.4	641.7363	21	100084.5	0.54

Table 3: An Example Set of Performance Data for the Critically Limited Engine, MR=2.625, 5 km trajectory

Of all three NTP engines, the Critically-Limited engine produced the least-satisfactory performance due to the smaller amount of thrust the engine produces. Since the lander was designed as a single stage, unmanned robotic lander with scientific instruments, it was viewed a primary candidate considering its low mass and low thrust that could yield better performance. It completed the smallest number of hops for all three travel distances. For the 5 km, 10 km and 25 km trajectories it completed a maximum of 21,10,6 hops respectively. All h_{ratio} values tended to high with values ranging from 0.54-0.6. This is due to the engine being under-powered in the lunar environment for this specific application. The results yield that if a lunar hopper is to be designed, it must have a greater thrust (34,000 N) or a smaller engine mass (1700 kg) to complete a greater number of completed hops. The Critically-Limited engine, though could potentially be suitable candidate for a smaller celestial body such as Phobos or Pluto, does not yield the best results for a lunar hopper.

MR	Mi	Mf	Apogee (m)	Restart Altitude(m)	Number of completed hops	X distance traveled for specfic hop (m):	h_ratio
3.375	11812.5	11544.78	992.718	416.9416	1	4971.894	0.42
3.375	11812.5	11254.2	1020.364	428.5528	2	5043.791	0.42
3.375	11812.5	10958.85	1020.678	428.685	3	4993.981	0.42
3.375	11812.5	10659.48	1021.084	428.8552	4	4944.706	0.42
3.375	11812.5	10350.66	1057.788	444.2709	5	5070.805	0.42
3.375	11812.5	10034.58	1060.697	445.4926	6	5025.814	0.42
3.375	11812.5	9710.487	1064.475	447.0796	7	4982.733	0.42
3.375	11812.5	9391.176	1069.389	449.1433	8	4960.921	0.42
3.375	11812.5	9068.188	1071.99	450.2358	9	4916.379	0.42
3.375	11812.5	8743.078	1074.476	451.2799	10	4872.016	0.42
3.375	11812.5	8417.758	1076.369	452.075	11	4826.989	0.42
3.375	11812.5	8080.007	1126.852	473.2779	12	4993.81	0.42
3.375	11812.5	7749.956	1132.503	475.6514	13	4973.702	0.42
3.375	11812.5	7422.945	1134.379	476.4391	14	4928.606	0.42
3.375	11812.5	7103.726	1133.685	476.1476	15	4879.357	0.42
3.375	11812.5	6789.447	1128.379	473.9192	16	4804.268	0.42
3.375	11812.5	6471.758	1184.281	497.3981	17	4997.4	0.42
3.375	11812.5	6163.187	1176.997	494.3387	18	4918.463	0.42
3.375	11812.5	5863.621	1163.229	488.5561	19	4810.923	0.42

3.375	11812.5	5563.208	1220.192	512.4805	20	5004.977	0.42
3.375	11812.5	5279.817	1199.593	503.8291	21	4885.209	0.42
3.375	11812.5	5011.487	1166.482	489.9222	22	4709.424	0.42
3.375	11812.5	4740.404	1212.784	509.3695	23	4847.278	0.42
3.375	11812.5	4475.33	1265.945	531.6967	24	5033.73	0.42
3.375	11812.5	4229.609	1213.435	509.6425	25	4787.881	0.42
3.375	11812.5	3988.341	1254.162	526.7481	26	4915.837	0.42
3.375	11812.5	3751.593	1296.467	544.5159	27	5047.157	0.42
3.375	11812.5	3535.513	1209.003	507.7814	28	4671.194	0.42

Table 4: Example Performance Data for the SNRE Engine, MR=3.375, 5 km trajectory

MR	**Mi**	**Mf**	**Apogee (m)**	**Restart Altitude(m)**	**Number of completed hops**	**X distance traveled for specific hop (m):**	**h_ratio**
4.125	18562.5	18116.61	982.9298	442.3184	1	4977.586	0.45
4.125	18562.5	17650.8	986.6596	443.9968	2	4933.792	0.45
4.125	18562.5	17184.54	992.4607	446.6073	3	4913.33	0.45
4.125	18562.5	16698.32	1030.233	463.6047	4	5041.551	0.45
4.125	18562.5	16204.62	1038.922	467.5149	5	5025.921	0.45
4.125	18562.5	15702.66	1048.174	471.6784	6	5011.401	0.45
4.125	18562.5	15174.4	1058.177	476.1795	7	4979.117	0.45
4.125	18562.5	14649.64	1072.154	482.4695	8	4992.336	0.45
4.125	18562.5	14134.24	1044.34	469.9532	9	4804.236	0.45
4.125	18562.5	13592.7	1095.982	493.1917	10	4973.542	0.45

4.125	18562.5	13068.91	1066.142	479.7639	11	4783.248	0.45
4.125	18562.5	12548.37	1075.212	483.8456	12	4769.758	0.45
4.125	18562.5	12035.87	1082.836	487.2763	13	4753.871	0.45
4.125	18562.5	11509.06	1140.567	513.2552	14	4950.792	0.45
4.125	18562.5	10988.94	1150.534	517.7401	15	4938.632	0.45
4.125	18562.5	10468.14	1158.057	521.1255	16	4903.936	0.45
4.125	18562.5	9963.586	1164.661	524.0976	17	4886.27	0.45
4.125	18562.5	9472.687	1165.697	524.5637	18	4840.852	0.45
4.125	18562.5	8994.621	1161.098	522.4942	19	4768.029	0.45
4.125	18562.5	8536.542	1150.347	517.6559	20	4685.014	0.45
4.125	18562.5	8074.761	1210.332	544.6495	21	4882.609	0.45
4.125	18562.5	7637.705	1191.936	536.371	22	4768.303	0.45
4.125	18562.5	7200.267	1252.601	563.6705	23	4967.25	0.45
4.125	18562.5	6795.407	1221.163	549.5234	24	4812.261	0.45
4.125	18562.5	6390.544	1276.29	574.3305	25	4983.415	0.45
4.125	18562.5	6016.397	1224.163	550.8735	26	4740.109	0.45
4.125	18562.5	5653.512	1269.955	571.4796	27	4893.888	0.45
4.125	18562.5	5296.39	1315.981	592.1913	28	5031.168	0.45
4.125	18562.5	4978.474	1224.223	550.9005	29	4650.184	0.45
4.125	18562.5	4671.273	1245.169	560.326	30	4706.767	0.45

Table 5: Example Performance Data for the Peewee Engine,MR=4.125, 5 km trajectory

Target Distance (km)	Engine	Dry Mass (kg)	MR	Loaded Mass	Number of hops completed	Minimum Restart Altitude(m)
5 km	SNRE	3500	3.0	10500	27	397
5 km	**SNRE**	**3500**	**3.375**	**11812.5**	**28**	**416**
5 km	Peewee	4500	3.0	13500	30	345
5 km	Peewee	4500	3.375	15187.5	30	385
5 km	Peewee	4500	4.875	21937.5	30	929
10 km	SNRE	3500	3	10500	17	737
10 km	**SNRE**	**3500**	**3.375**	**11812.5**	**16**	**847**
10 km	SNRE	3500	4.125	14437.5	16	971
10 km	Peewee	4500	2.625	11812.5	18	622
10 km	Peewee	4500	3	15187.5	19	857
25 km	SNRE	3500	3.0	10500	9	1943
25 km	**SNRE**	**3500**	**3.375**	**11812.5**	**9**	**2012**
25 km	Peewee	4500	2.625	11812.5	8	1699
25 km	Peewee	4500	3.0	15187.5	10	1610
25 km	Peewee	4500	3.375	11812.5	10	1784

Table 6: Highlighted MR's and Engine Combinations for the SNRE and Peewee Class Engines

3.3 SNRE and Peewee Performance

The SNRE and Peewee Engines were more comparable in performance and yielded results that completed more hops than the Critically Limited engine. The vehicles tended to more similar performance for trajectories that feature a larger horizontal travel distance. Table 6 displays a very convenient list of results that are at or near the maximum number of hops for both the

Peewee Engine. The SNRE with its 3500 kg dry mass was able to attain for the 5 km, 10 km, 25 km trajectories a maximum of 28, 17 and 9 hops respectively. The Peewee Engine with its 4500 kg dry mass was able to attain for the 5 km, 10 km, 25 km trajectories a maximum of 30, 19 and 10 hops respectively. For both landing configurations, the h_{ratio} typically favored values of approximately 0.4-0.45 for all three trajectory types.

The SNRE and Peewee were able to attain higher Apolunes and had consistently lower restart altitudes than the Critically Limited, since the engines produced more thrust by a factor of ~2 and ~3 respectively.

One will notice that there are multiple repeating MR's that are featured for all three types of trajectories. MRs 3.0 and 3.375 have also produced a high number of hops in all three of the trajectory categories for both lander configurations.

Originally a 100 km trajectory was analyzed and integrated into this study, however it was left out of the report since the landers completed much fewer hops (0-2 on average) of that category and the SNRE and Peewee landers yielded almost identical performance in terms of the number of hops being completed. This is due to the engine burning for a greater amount of time (2-3 additional minutes compared to the 25 km case) to meet the horizontal target requirement and decelerate the hopper to land at safe velocities. Differences in engines, dry masses and MRs matter more for shorter hops based on the shorter time traveling in flight. It takes acceleration (~200-250 m/s to 0 m/s and 2 m/s for Vx and Vy respectively) to safely land the vehicle, which is why the data from the 5 km, 10 km and 25 km were show-cased in the report and used to stratify the designs against each-other.

3.4 Selecting the Design

Considering theoretical number of hops alone, the Pewee configuration completed the greatest number of hops for all three trajectories simulated.

Design philosophy must focus on limiting mass and volume while maintaining the flexibility to achieve this mission on commercially available launch vehicles. New launch vehicles currently

in development such as Blue Origin's New Glenn or SpaceX's Starship will have the capability to deliver the vehicle to the lunar surface, while offering more payload volume for a lander carrying 8000+ kg of liquid hydrogen.

The rocket equation is governed primarily by mass ratio and exhaust velocity. The more mass means more volume must be taken up. The propellant being used, LH2, is the lightest possible rocket propellant, and subsequently has a low density. As more propellant mass is added to the vehicle, more volume must be taken up (substantially more than for other propellants such as LOX or RP-1). Launch vehicle fairing volume introduces an additional constraint; if the vehicle cannot physically fit inside of the fairing it cannot be launched.

The vehicle must land on the surface with enough propellant remaining for hops. It is also desirable to minimize the transfer time from LEO to the lunar surface to ensure the propellant doesn't boil off into gaseous hydrogen while transiting. Previous unmanned lunar lander missions (Beresheet, Chandrayaan-1) utilized electric ion thrusters taking advantage of the high Isp that these offer. However, the major disadvantage is that the low thrust of these propulsion systems means the vehicle will spend a lot of time in high earth orbit. The landers that utilized this spent 45 days orbiting the Earth using low-impulse burns to eventually insert itself in lunar orbit. The possibility for a second booster with an engine that can deliver a high impulse should be also considered in the design as an effective way to deliver the hopper to its first landing-site, further emphasizing the desire to decrease mass where possible.

While the Peewee completed the most hops, SNRE was very close to matching its performance typically completing only 1-2 less hops in a given category. The larger mass means larger size and for a project that would feature new and unproven hardware systems means added complexity that can lead to higher costs. The Peewee designs would potentially be an excellent continuation in the NTP hopper series but starting small would likely be beneficial so the basic concept can be proven before more ambitious risks are taken.

For these reasons, the SNRE with an MR of 3.375, a fully loaded mass of 11812.5 kg and a base mass of 3500 was selected for the final design.

3.5 Maximizing Performance

The limitation of the primary results is that they do not show the maximum potential of the hopper. The h_{ratio} remains constant for each iterative cycle, which sets a limitation. As fuel depletes and mass of the spacecraft decreases, the acceleration of the vehicle increases. This means that the optimum altitude for restart for powered descent is lowered for every hop as the vehicle can afford to wait longer to restart the engine and produce enough acceleration to slow the lander in time to gently touch the surface. Thus, the second round of simulations was integrated with a more refined code that started powered descent at the most ideal moment. This ensured the vehicle could land safely on the surface without depleting fuel unnecessarily by beginning powered descent too early. This was not done for the first round of simulations for the fact it would have added unnecessary complexity to try and figure out the proper combination for each individual engine, dry mass and MR.

For these continued runs of the simulations, as the vehicle completed more hops the restart altitude was lowered, and more fuel was conserved on-board. These restart altitudes are custom to each engine, MR and final mass combinations. The results were greatly improved as the number of hops increased by a factor of ~1.5-2 in each category as shown by Table 7. Note that the 4500 kg dry mass was tested as well the SNRE to measure the decrease in performance if certain subsystems will require more mass for the vehicle to be fully functional. This data will be referenced again in the “Final Vehicle Performance Chapter.”

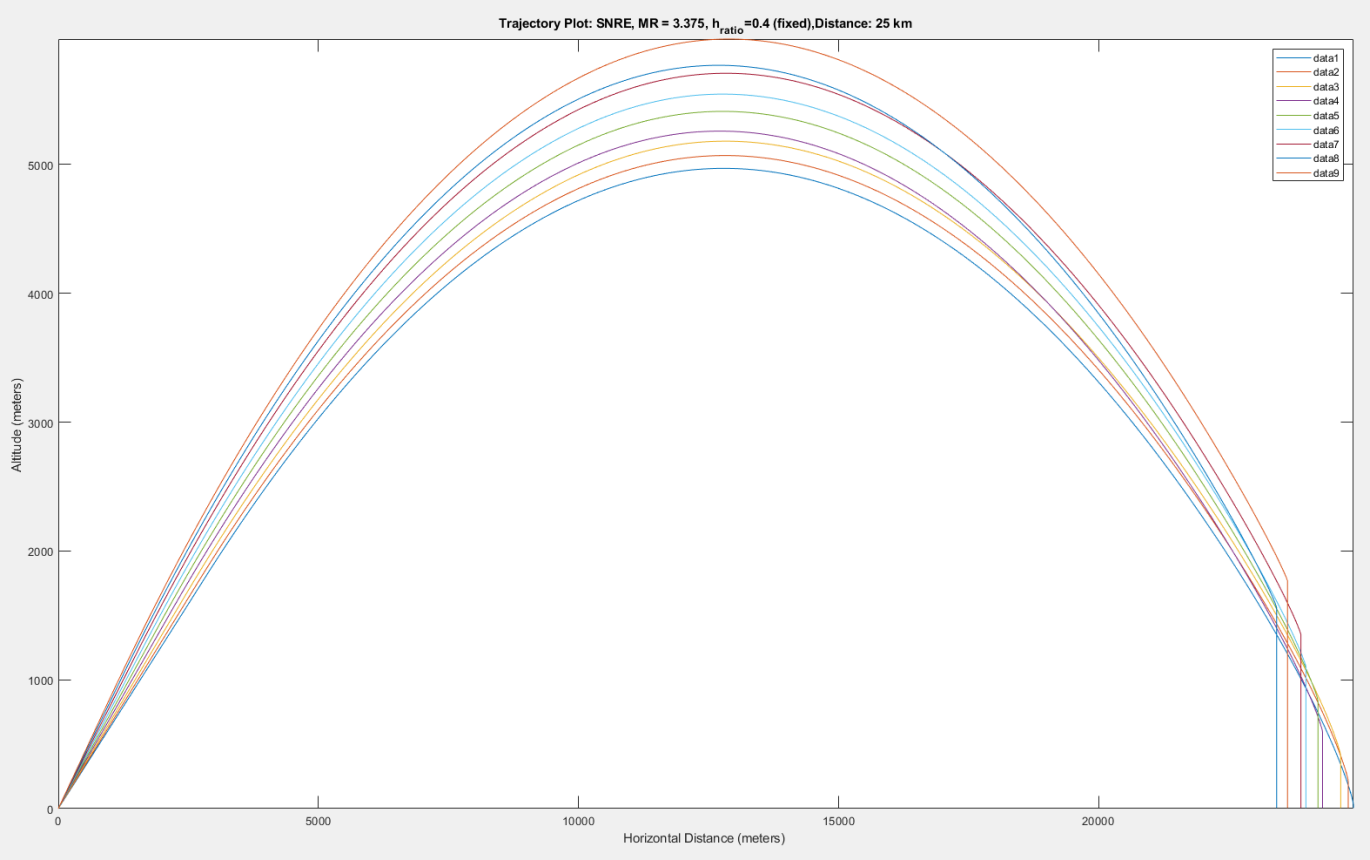

Figure 13: Initial Trajectory Plots

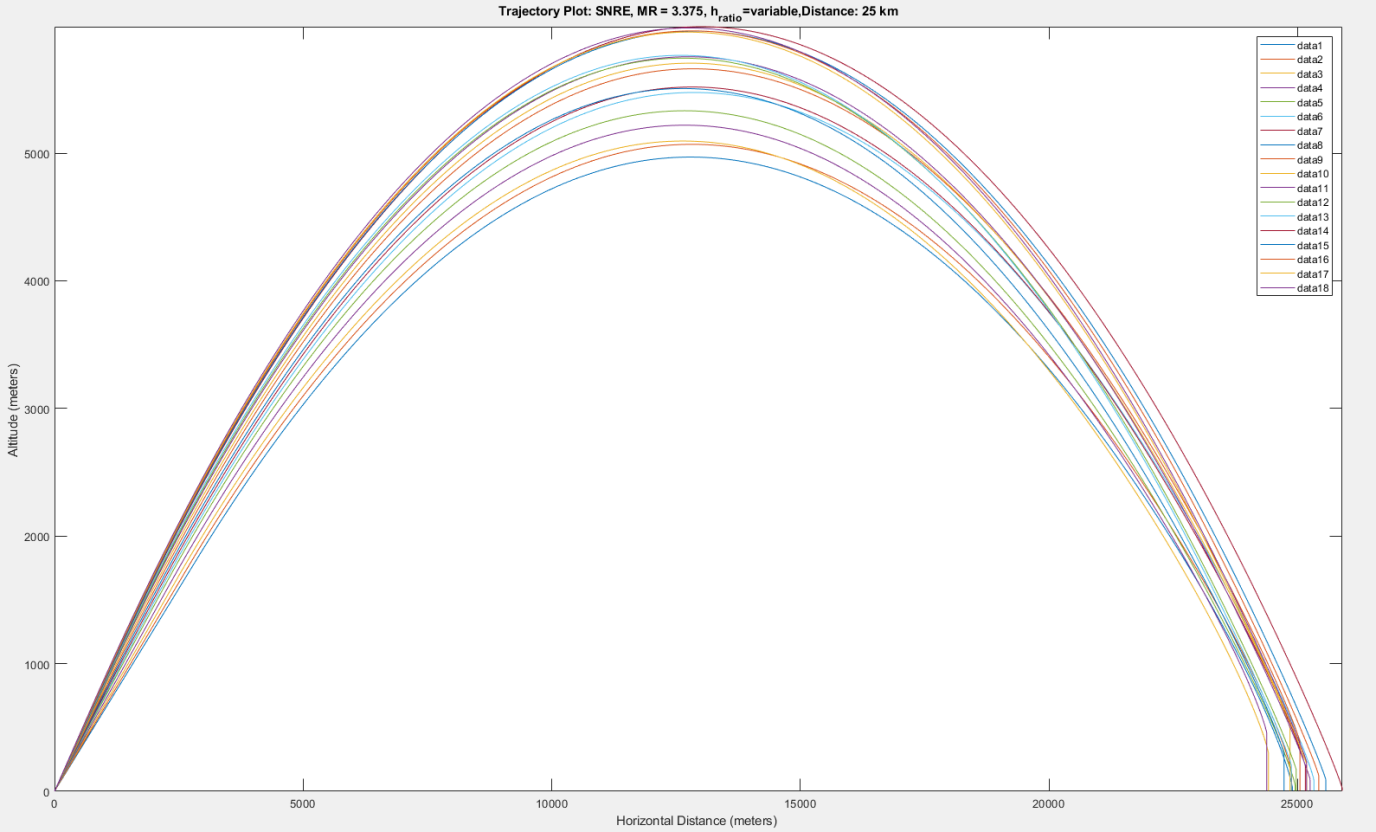

Figure 14: Refined Trajectory Plots

Trajectory Type (km)	Maximum Number of hops
5	39
10	31
25	16

Table 7: Maximum Number of Hops for SNRE, MR=3.375, Dry Mass: 3500 kg

Trajectory Type (km)	Maximum Number of hops
5	35
10	24
25	12

Table 8: Maximum Number of Hops for SNRE, MR=2.625, Dry Mass: 4500 kg

Chapter 4 - Design

4.1 Initial Sizing of the Vehicle

Using the SNRE, MR=3.375 design the design is based on the Propellant Mass that needs to be carried. The mass is calculated by subtracting the total mass from the target weight. The volume of the propellant is then calculated by taking the mass of the propellant and dividing by the density.

$$Mass_{\,Propellant} = 11812.5 - 3500 = 8312.5\ kg \quad (4.1)$$

$$Volume_{\,Propellant} = \frac{Mass_{\,Propellant}}{LH_{2}\ Density} = \frac{8312.5\ kg}{70.8\ \frac{kg}{m^3}} = 117.43\ m^3 \quad (4.2)$$

The largest possible diameter offered by new, upcoming launch vehicles was selected in order to decrease static and dynamic instability for when the lander touches down on the lunar surface. Choosing the maximum possible diameter, decreases the risk of the vehicle toppling over.

A Launch vehicle that can meet both the volume constraints and gives enough performance with specific energy (C_3) that it can insert the lander directly into TLI is highly desired.

Blue Origin's New Glenn Launch Vehicle is highlighted as a possible contender with its large diameter for carrying payloads and its performance. The vehicle can lift ~41,000 kg into LEO and ~12,000 kg into GEO for a two-stage configuration with a reusable first stage ("New Glenn", n.d.). The company is currently working on a three-stage configuration which should deliver even better performance based on the increased Delta-V that would be provided. While the exact TLI mass is unknown and it is not known if the company plans on offering the first stage to be expendable, it appears that it would be feasible to launch the hopper on the vehicle with a possible second stage to land on the lunar surface directly based on given data and historical comparison to other launch vehicles ("New Glenn", n.d.). More importantly, it offers a 7 m

diameter fairing which far surpasses that of any other launch vehicle that is currently operational.

SpaceX is also developing a more powerful vehicle, known as Starship, that offers a 9 m fairing and 100,000 kg+ TLI, contingent upon orbital refueling capability in LEO (“Starship”,n.d.) Given this capability that the next generation launch vehicles will offer, the lander’s diameter was specified as 6 meters. This will leave sufficient room to take full advantage of mission flexibility from commercially provided options that should be coming online within 3-10 years. Given that the lander described here is only a notional design to be used as a part of early studies, several simplifying assumptions were made in order to project a visualization of components

and technologies that need to be fully developed, tested and integrated together.

4.2 Design Layout

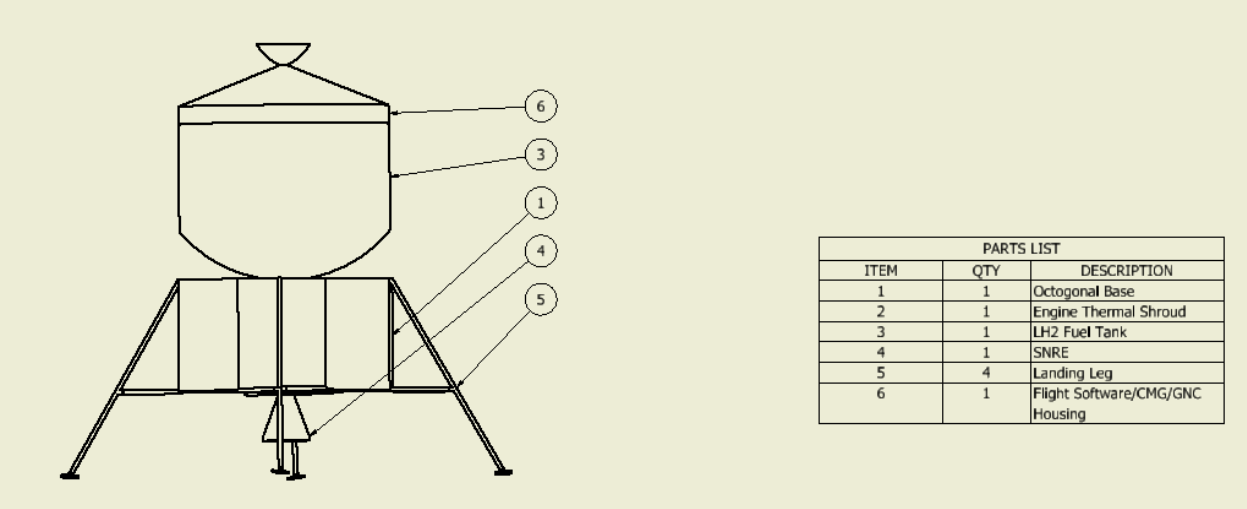

PARTS LIST		
ITEM	QTY	DESCRIPTION
1	1	Octogonal Base
2	1	Engine Thermal Shroud
3	1	LH2 Fuel Tank
4	1	SNRE
5	4	Landing Leg
6	1	Flight Software/CMG/GNC Housing

Figure 15: Ballooned Drawing of the proposed Lunar Hopper

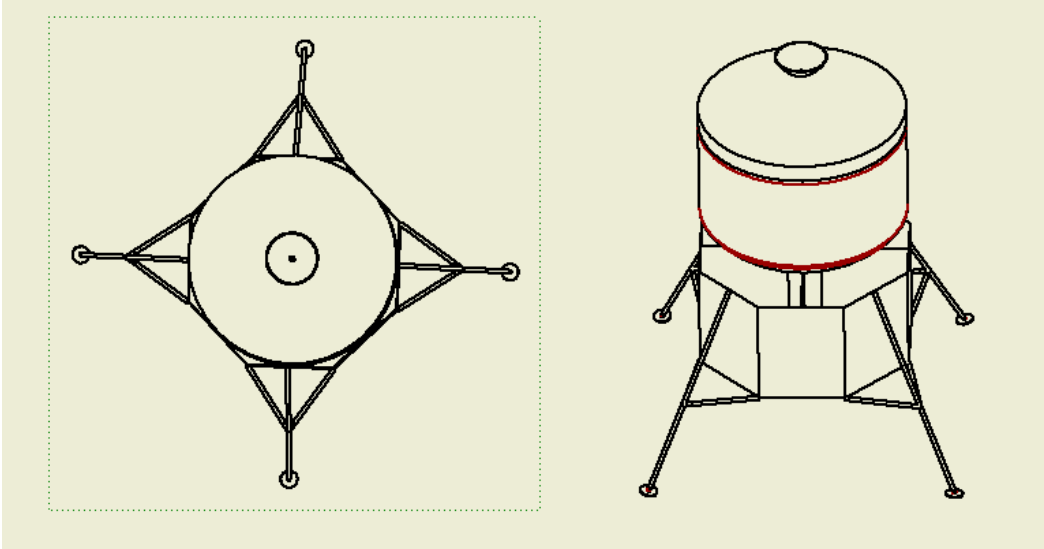

Figure 16: Vertical views of the hopper looking down on the Spacecraft

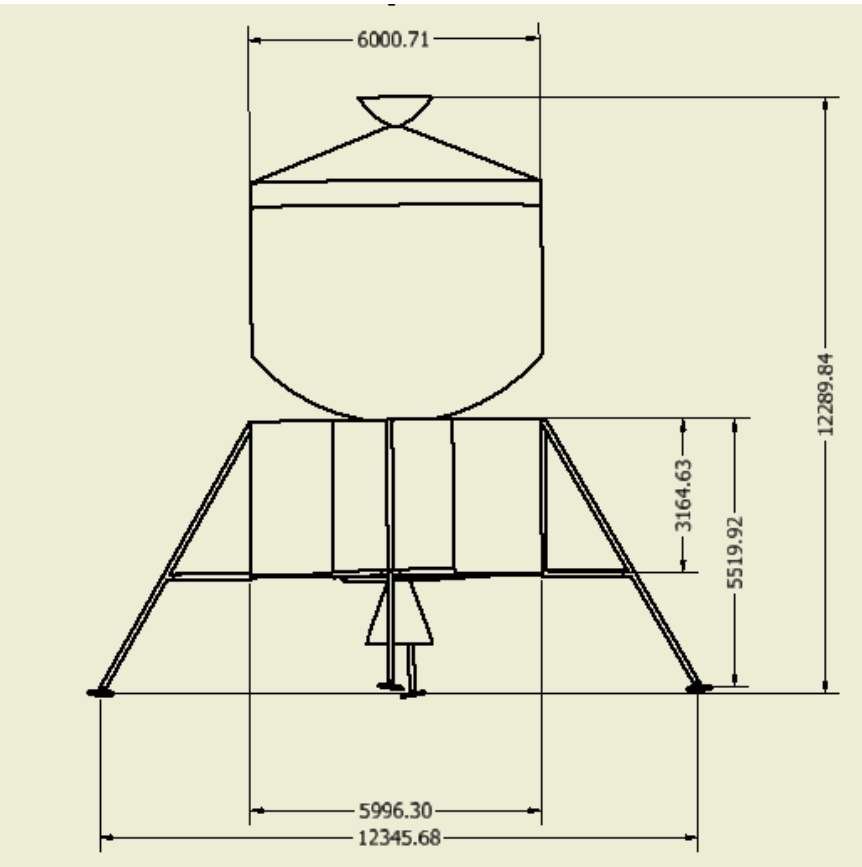

Figure 17: Drawing of Lander with units (mm)

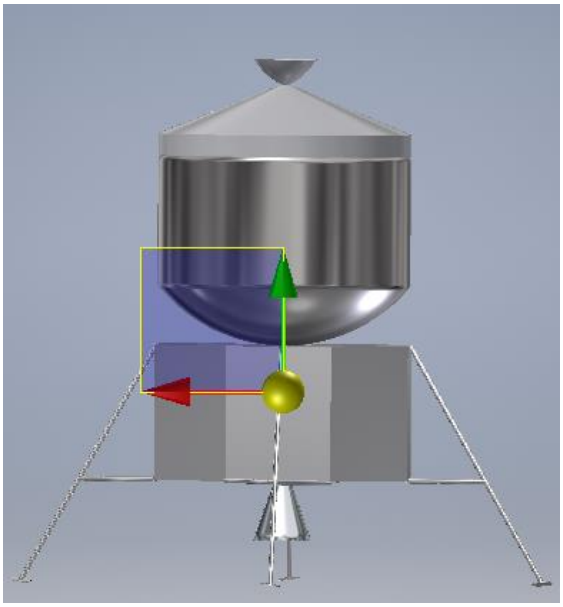

Figure 18: 3D-Graphic Highlight the Location of the Center of Gravity (no propellant on board)

Mass Properties

Component	**Mass (kg)**
Fuel Tank (Stainless 301, Composite)	419.1 kg/71.88 kg
Lander Base Chassis (Aluminum 7075)	65.27 kg
Landing Legs (Aluminum 7075)	300 kg
SNRE Engine	2400 kg
Pressurization Systems	10 kg
Engine Heat Containment System	65 kg
Communications	41 kg
Batteries/Related Power Management	153.35 kg
Thermonuclear Generator	20 kg
Solar Panels	10 kg
Control Moment Gyroscopes	88 kg
Flight Computer and Autonomous Landing System	100 kg
Scientific Payloads/Instrumentation	100 kg
Multi-Layered Thermal Protection System	300 kg
Total Mass	**4071.1 kg/3724.5 kg**

Table 9: All Mass Properties of Relevant Subsystems

The primary focus of the physical design was to focus around the volume LH_2 that needed to be supplied to achieve the desired mass ratio. The design of the tank included a symmetric design with respect all 3 axes. that can carry 117.43 m^3 of LH2. Not show in the drawing but the tank will be supported by a truss connected to the lander base. The tank has a selected diameter of 6 m and a height of 4.8 m. All the individual drawings of the components can be found in the Appendix. The center of gravity (for an empty vehicle) is measured to be centered in the X-Z axes and on the Y-axis, it is measured 4.65 meters from the bottom of the landing legs. Further studies will be conducted in future to verify stability and the center of gravity location for when the vehicle is loaded with fuel.

4.3 Structures

Two different materials were selected for analysis: Stainless Steel 301 and Carbon Composites. For this study, an existing space vehicle that utilized LH2 was selected as a starting point. The Centaur upper stage was selected for its historical use of a LOX/LH2 booster that was specifically designed for in-space (non-atmospheric) operations. According to original NASA Technical Memorandums, the booster utilized a thickness of approximately 0.014 inches for most of the tank (NASA TM X-1844, 1970). The units were then converted into SI and used for the CAD file.

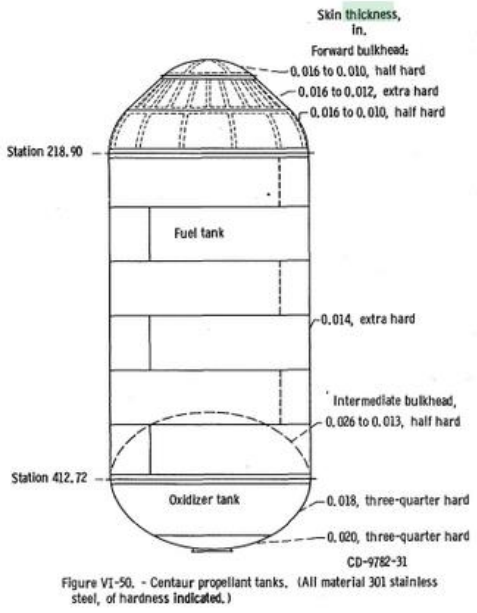

Figure 19: Schematic of Centaur Fuel Tank (NASA TM X-1844, 1970).

The advantage of SS-301 is that it has been utilized in industry for many decades and a lot is known about working with the alloy. It features a high strength to weight ratio which is critical for a vehicle that must minimize dry mass as much as possible.

Another alternative is carbon composites. The advantage of utilizing carbon composites is that it has a comparable strength to weight ratio but has approximately only one fifth of the density of steel. This leads to considerable mass savings which increase the number of hops the lander would be able to complete.

Significant work has been done on composite tanks since the 1980s with NASA programs such as *Delta Clipper* and the *X-33* that built, developed and tested prototype LH2 composite tanks (Zheng, Zeng & Zhang, 2018). SpaceX also built and tested a prototype composite fuel tank for their envisioned *Interplanetary Transport System* back in 2016 (Zheng et al, 2018).

Resulting tests and studies shows that if employed correctly, carbon composites can handle similar stresses and loads as any sort of aluminum or steel alloy (Zheng et al, 2018) . The technology has yet to be fully developed, however, as there are still technical problems to deal

such as dealing with permeation and the material becoming more brittle at cryogenic temperatures.

4.3.1 Main Chassis/Scientific Bay

The landing chassis was designed primarily to support the LH2 fuel tank, engine mount and landing legs. Detailed structural design is beyond the scope of this study, so as many lessons learned possible were borrowed from the Apollo LM since the scale is similar in terms of mass. The first commonality is the shape as it shares the same octagonal shape.

The Apollo LM descent stage was originally designed with a round/ circular descent stage, but it evolved to the octagonal shape as structural test articles found that it would better support impacting the lunar surface (Hero's Relics, 2019).

Rather than use an octagonal truss, the panels were chosen to provide to provide storage and shelter from the radiation from the engine and lunar dust particles kicked up from the landing that could contaminate sensitive scientific payloads and experiments.

The next commonality is the material. Aluminum was chosen as the material of the octagonal body due to its lightweight characteristic while also having enough tensile strength to support the weight of the fuel tank. The Apollo LM Descent stage had shear panels act as diagonal-tension field beams. Vertical panels had a thickness of 0.006 in while top panels had a minimum thickness of 0.012-0.015 in (Weiss, 1973).

The chassis can either be milled, tig-welded together using sheet metal or possibly metal 3-D printed.

It is important to note the differences in the loading from the hopper to the Lunar Module. The Apollo LM had two-thirds the weight in the decent stage, while most of the mass for the hopper is in the top half of the vehicle with the LH2 fuel tank. For this reason, the thickness for the vertical panels were doubled to 0.012 in of the LM Descent Stage so it would provide better

support to 8712.5 kg of fuel and structure (the LM Ascent stage weighed around 5300 kg.) The Fuel Tank would be supported vertically with a truss system (not shown in drawing) instead of using top panels like the LM did. This decision was made since the hopper is single stage and the bottom-half of the vehicle won't serve as a launch pad for an ascent element. Inside of the panels are 4 walls that form the boundaries for the boundaries of 4 internal bays that can be used for storage of payload and electronics that connect to a circular shaft that will hold the engine.

The shaft features an aluminum base that has a layer of titanium within it and a layer of insulation to keep the heat of the engine (367 Megawatts of Thermal Power) from damaging the aluminum structure (Borowski & McCurdy, 2017).

Validating the main structure of the hopper, the axial loading is analyzed referencing the compressive stress of Aluminum 7075. The focus is on this component of the lander for validation since it will hold most of the load, from both the weight of the fuel tank and from the engine when operating. The values are well below the yield strength of Aluminum 7075 ("ASM Material Data Sheet", n.d.) The parameters calculated are the axial loading from the fuel tank (on earth) and the thrust of the engine at full throttle. These are compared to the ultimate and fatigue stress of the material.

$$\sigma_{weight-fueltank-Earth} = \frac{W_{fueltank}}{A_{cross-section}} = \frac{8312.5\ kg * 9.8\ \frac{m}{s^2}}{0.007\ m^2} = 11.64\ MPa \quad (4.3)$$

$$\sigma_{Thrust} = \frac{Thrust}{A_{cross-section}} = \frac{74{,}000\ N}{0.007\ m^2} = 10.57\ MPa \quad (4.4)$$

$$\sigma_{ulimate-yield} = 572\ MPa \quad (4.5)$$

$$\sigma_{fatigue} = 159\ MPa \quad (4.6)$$

4.3.2 Landing Gear

The mass of the landing gear was approximated to be 2.5% of the total mass of the hopper based on data from the Apollo LM and other experimental studies regarding this specific topic (Weixong, 2017). The landing system was also designed to be made from aluminum components; however, the actual system will be needed to be designed with reusability since multiple hops. For a conceptual design, this estimate will be sufficient for this study.

The Apollo LM and other unmanned landers such as a Viking have only utilized and designed landing gear for one-time use. Many landers utilized honeycomb absorbers that “crushed” upon impact with the surface. It features a simple and effective means of dealing with the loading from touchdown, but it will not be suitable for the case of a hopper that has to land and take off repeatedly.

The final design of the lander gear will likely require some sort of multiple-use shock absorber. Some designs have been created and proposed in this specific case with the three main methods: metal bellows, electromagnetic, and electromechanical (Weixong, 2017).

Further analysis will need to be done on fatigue to ensure the landing support system can handle more loads. It is very possible that the overall mass of the structure will need to be increase in order to support the weight of the vehicle, the thrust from the engine and the impact from completing numerous hops on the lunar surface, which might risk hindering the vehicle performance.

4.4 Engine

Typically, for applications of in space-propulsion pressure fed engines are used because they tend to be simpler and more reliable compared to turbopump engines. Thrust is determined primarily by chamber pressure and temperature. One of the reasons why an NTP engine is so efficient is because it can achieve a relatively high temperature using nuclear fission instead of a chemical reaction and the low atomic number of the propellant. Despite the high temperature the reactor can produce, the chamber pressure still needs to be high in order to achieve a

relatively high amount of thrust. All NTP engines built or tested have used either closed or open cycle turbopump engine to yield the sort of chamber pressures needed.

The LH2 tank is pressurized using helium gas. Referencing sizing equations for LOX/LH2 boosters, it is estimated that the volume and mass of the tank will be 0.1 m^3 and 10 kg respectively (Atkins, 2016).

This is beneficial to the design, in part because the LH2 tank can be kept lightweight (more pressure, means a thicker structure is needed). However, for this hopper configuration multiple restarts are required.

Turbopumps must be designed to handle stress and while they typically preform as expected for a single firing, the probability of failure increases for every restart in space. This topic will be further explained in a later section.

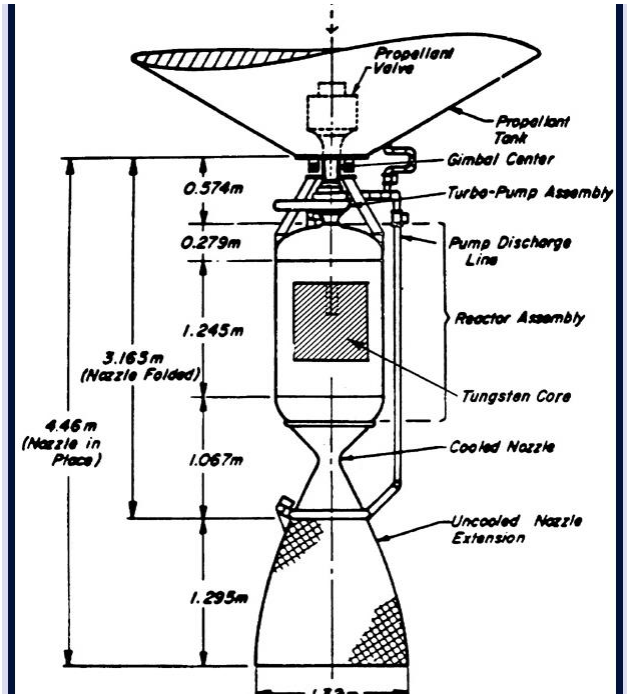

Figure 20: Schematic of a SNRE used for the CAD model (Project RHO: Engine List 2, n.d.)

4.5 Controls

Because minimizing mass is a primary constraint on the design, RCS and related propellants were seen to be not satisfactory for this application. If a spacecraft is going to produce 10+ hops and will need a large volume of heavy, dense monopropellant, the overall performance of the vehicle would suffer due to the lower MR. Thus, reliance on Control Moment Gyroscopes seemed a better design choice: using power to steer the spacecraft.

The Honeywell M160 was selected with each model weighing 44 kg and consuming 217 watts of power (Leve, 2009). The CMG offers a torque of 216.93 Nm. Two CMGs will be utilized in order to ensure redundancy if one fails. The minimum amount of time for engine restart is referenced for a 1000 meter trajectory of which the lander will have approximately 18 seconds to reorient itself in a retrograde direction. The rotation is will be approximately 90-120 degrees looking at the spacecraft in a 2-D Frame.

With the corresponding moments of inertia of the lander being: Ixx=Izz=17750 kg m^2 and Iyy=7220 kg m^2 in a period of ten second it can rotate the lander a maximum of 68.64 degrees on the x and z axis and 385.42 degrees on the y axis.

$$I_{xx} = I_{zz} = 17750\ kg\ m^2 \quad (4.7)$$

$$I_{yy} = 7220\ kg\ m^2 \quad (4.8)$$

$$\tau_{max} = 432\ Nm \quad (4.9)$$

$$\tau_{x\_Max} = \tau_{z\_max} = I_{zz}\alpha_z = I_{xx}\alpha_x \quad (4.10)$$

$$\tau_{y\_Max} = I_{yy}\alpha_y \quad (4.11)$$

$$\alpha_{zmax} = \alpha_{xmax} = 0.0243\ \frac{rad}{s^2} \quad (4.12)$$

$$\alpha_{ymax} = 0.0598\ \frac{rad}{s^2} \quad (4.13)$$

$$\Delta\theta = \theta_0 + \omega_0\Delta t + \frac{1}{2}\alpha\Delta t^2 \quad (4.14)$$

$$\theta_0 = \omega_0 = 0 \quad (4.15)$$

$$\boldsymbol{\Delta t = 5\ sec} \quad (4.16)$$

$$\Delta\theta_{x,zMAX} = 17.6 \text{ degrees} \quad (4.17)$$

$$\Delta\theta_{yMAX} = 42.85 \text{ degrees} \quad (4.18)$$

$$\boldsymbol{\Delta t = 10\ sec} \quad (4.19)$$

$$\Delta\theta_{x,zMAX} = 68.64 \text{ degrees} \quad (4.20)$$

$$\Delta\theta_{yMAX} = 171.4 \text{ degrees} \quad (4.21)$$

$$\boldsymbol{\Delta t = 15\ sec} \quad (4.22)$$

$$\Delta\theta_{x,zMAX} = 155.32 \text{ degrees} \quad (4.23)$$

$$\Delta\theta_{yMAX} = 385.42 \text{ degrees} \quad (4.24)$$

Thrust vectoring/gimballing might also be a considered added benefit to help better control the lander during ascent and powered descent. Thrust vectoring would likely require a redesigned support system for the engine which will in-turn add more mass and complexity. More trade studies must be completed in order to determine if thrust vectoring would be a worthwhile investment.

4.5.1 Computer, Avionics and GNC

NASA programs such as Project ALHAT and COBALT have developed and tested the next generation of GNC algorithms for lander vehicles. Both programs have focused on integrating a hazard detection system composed of lidar doppler radar, lasers and sensor technology for the vehicle to autonomously land safely with pinpoint precision. ALHAT was able to demonstrate this technology on a Bell UH-1 Helicopter and a prototype hopper called Morpheus (Crain, Bishop, Carson, Trawny, Sullivan, Christian, J. A., … & Hana, 2016). Project COLBALT was a continuation from ALHAT and demonstrated the new emerging technologies on a lander named *Xodiac* built by Masten Space Systems. The vehicle featured a system of Navigation Doppler

Lidar cameras integrated with an IMU and a Computing Element to have the vehicle ascend 530 m and land autonomously to a spot 300 m away (Carson, Seubert, Amzajerdian, Bergh, Kourchians, Restrepo, … & Garcia, 2017).

The final GNC and Flight Software products that came from ALHAT and COLBALT would be a suitable match for the hopper being designed once they become flight certified and ready for practical use. The payload mass of the *Xodiac* was approximately 50 kg; for this example, it was doubled to account for any additional lidar cameras or processors that would need to be added.

4.6 Communications

The lander will communicate to the control-station on Earth using S-band and Ku-band frequencies. Detailed design of the communications subsystem is beyond the scope of this study. To maintain the focus of the mass and volume of components, two common systems were used as a reference from Larson and Wertz's *Space Mission Analysis and Design (2019)* and have been chose to be integrated into this conceptual design (Larson & Wertz, 1997, pg. 444.)The mass of the S-band and Ku-band systems are 28.54 kg and 13.3 kg respectively. More detailed analysis on the communication requirements will be completed in later studies.

4.7 Power

Most of the power will be supplied with the Nuclear Reactor. The thermal power generated from the reactor is 367 Megawatts (Borowski & McCurdy, 2016). Even with the efficiency of thermoelectric generators being only 3-7% efficient, there is an abundance of energy to run the spacecraft's electrical needs (Chen, Wu, Lang & Lin, 2016). Bimodal NTPs were not chosen for the sake of all propellant being used to produce thrust, not electrical power. The overriding design objective for this project is to visit as many landing-sites as possible.

The electrical budget was based on the hardware inputs (Masten for the Xodiac Payload, Honeywell for CMGs, etc) from the suppliers. The scientific payloads were given a budget of

250 W based on what the *Curiosity Rover* had, but increased by a factor of 6 to accommodate several experiments or instruments (drills, robotic arms, etc.) Note that the wattage for the scientific payload is treated different as during powered flight it will be in an idle state compared to the other systems. The NiH2 was chosen for its recharge capability and high capacity. It was desired that the batteries could support scientific experimentation and data collection (250 W) for 12 hours without any power generated. A small solar panel is installed while the engine is off so the risk of running out of power on the surface is minimized and to have some redundancy for means to produce electrical power.

Subsystem	**Power (Watts)**
CMG	258
Scientific Payloads	**250**
Pressurization	5
Flight Software/IMU	500
Communications	81.8
Miscellaneous	100
TOTAL	944.8 W (Not counting Scientific Payload)

Table 10: Power Requirements for Subsystems

Average Time for 10 km trajectory→ 6 min → Round up to 10 min

$$944.8\ \text{W} * \ 0.1666\ \text{hrs} = \ 157.46 \ \ \text{Wh} \quad (4.25)$$

Scientific Bay

$$250\ W * 12\ hrs = 3000 \ \ \text{Wh} \quad (4.26)$$

Component	Power	Mass (kg)
Batteries (NiH2)	-	66.6
Power Control Unit	-	18
Regulators/Converters	190 W (consumed)	23.75
Wiring	28.5 W (consumed)	35
Solar Arrays	250 W (generated)	10

Table 11: Power Consumption and Mass (Larson & Wertz, 1997, p.334)

4.8 Thermal Systems

On the lunar surface heat flux will be experienced from solar radiation from the sun and not convection. Emphasis shall be focused on making sure that heat from the sun will not cause the LH2 to boil off. Likely the final design will require more insulative material wrapped around the fuel tank. Thus, the thermal protection system will utilize layers of thermal blankets and insulative materials to block away excessive heat from the sun to ensure that the metal structure won't receive substantial heating.

300 kg was chosen as a baseline number to start due to detailed thermal analysis being outside of the scope of this study. Trade studies will need to be completed to determine if the Mylar and Insulation will be enough or if radiation panels will be a good addition. More studies should also be completed to determine how the vehicles subsystems will be affected if the lander is exposed to lunar night for two weeks.

4.9 Concerns and Considerations

4.9.1 Zero-Boil-Off

The concept of using NTP for applications for Lunar Exploration does not come without limitations and disadvantages. One that the LH2 needs very little energy input to turn to gas. A propulsion expert at NASA Johnson Space Center has stated that LH2 can evaporate up to 2% by volume every day the vehicle is on the surface (E. Hulbert, personal communication, July 2019). Refueling of LH2 on the surface also poses several technical and logistical problems that need to be organized and solved. One viable solution is to integrate into the lander the capability of having a Zero-Boil off system (ZBO). The theory utilizes a Brayton Refrigeration cycle to constantly cool the inside of the tank to ensure that propellant remains liquid. It ensures that every gram of H2 is a usable liquid and funneled through the engine. More mass, support structure and radiation panels would need to be added, and further trade studies will be required before determining if integration will yield an increase in performance.

4.9.2 The Restart Problem

The main physical limitation of this proposal is with the issue of restarting the engine. Historically speaking, for in space propulsion most of the engine concepts have focused pressure-fed engines that are simpler and have higher reliability. However, pressure-fed engines are only applicable for engines that produce low/moderate thrust. Every NTP that has been built or theorized has utilized a turbopump in its cycle. Getting a high temperature thanks to the fission in the reactor is only a part of the solution. The chamber pressure must be high if one desires a high amount of thrust to exist. It physically challenging to make LH2 pressure based on the behavior of the propellant and how the weight of the tankage would have to increase in order to be handle very high pressures. Most explosions or failures during missions occur during (re)ignition when the turbopump is starting up and pumping fluid to the combustion/thrust chamber. This problem has never been fully solved as there hasn't been that much of need to stop and restart an engine that many times. If this hopper concept is to become

a reality, there must be more R&D that goes to study of material fatigue and weakness of performance with regards to turbopump performance and pressurization of tanks (E. Hulbert, personal communication, July 2019). In addition to this, LH2 is also difficult to work with as it tends to embrittle metal over time. More research and investment must be made into this as well to determine if an engine that will need a large number of restarts will need changes in its internal design for applications of pumps and plumbing.

4.9.3 Radiation Impact on Lunar Environment

Analysis should be conducted to determine how any type of lander integrated with NTP would affect the lunar atmosphere and surface. Environmental studies should be conducted to determine if the lunar hopper would pose a threat to any permanent moon base or settlement. If there is a concern that threatens life or science on the surface of the moon, engineering efforts must be focused on solving the problem and eliminating the radioactive particles from being a threat.

Chapter 5 - Final Vehicle Performance

45 degrees	Number of Hops (3724 kg)	Number of Hops (4071 kg)
1 km	79	74
5 km	27	21
10 km	16	15
25 km	8	8

Table 12: Table of Non-Refined Performance Data for a Dry Mass of 3724 and 4071 kg with a gamma1 of 45 degrees

60 degrees	Number of Hops (3724 kg)	Number of Hops (4071 kg)
1 km	71	66
5 km	24	23
10 km	14	13
25 km	6	6

Table 13: Table of Non-Refined Performance Data for a Dry Mass of 3724 and 4071 kg with a gamma1 of 60 degrees

Above are two tables containing the final trajectory data, with the two final conceptual dry masses (with the composite tank and SS-301 respectively). It is important to note that this reflects a “non-refined” restart altitude. This was done since the final dry mass will most certainly change when the project moves into the Preliminary Design Review and the hardware requirements are more refined. It would be better to do that analysis when the project continues further along in development.

Table 8, in Chapter 3 offers a refined set of data with the restart altitude optimally set for the SNRE integrated with a dry mass of 4500 kg. This was done to gage an extreme limit since it is a reasonable possibility the dry mass will increase up to 4500 kg to account for thermal shielding, reusable landing gear and other important subsystems. Overall there is a slight reduction in the number of hops being able to be completed, however the performance is

relatively unhindered. When comparing Table 7 and Table 8 the maximum decrease is in the 10 km category from 31 hops to 24 which is only a 23% decrease in the number of hops being able to be completed.

Chapter 6 - Conclusion

This research explored an overall preliminary concept: design a vehicle that can effectively survey the lunar surface, search for mineral deposits and help find locations where ISRU would aid in making human presence long term and sustainable by using NTP to “hop” to multiple locations. A vehicle was designed to maximize the number of sites it can visit based on one full-tank of propellant. Three different engines and dry mass combinations were tested among a list of possible mass ratios. A program in MATLAB was created so the optimum MR, engine and dry mass combination could be evaluated. Upon reviewing the data, the SNRE was selected with a target dry mass of 3500 kg. A proposed vehicle was designed based on the needed volume of LH2, the capability of new emerging launch vehicles and the size of the SNRE.

This conceptual design can be used as a starting point for more detailed engineering analysis on all the subsystems. Future work will entail: outlining the hardware requirements in detail, preforming Finite-Element Analysis on the structure, thermal analysis to determine the layers of insulation or number of radiation panels needed, investment into making turbopump engines more restart friendly, limiting the amount of mass where possible, refining the communication requirements for transmitting data, developing the landing gear, verifying the spacecraft is statically stable with the center of gravity, developing the control and computer algorithms needed and getting government or commercial partners on-board to make this vision a reality within the next five to fifteen years.

Appendix

Dimensioned Drawings

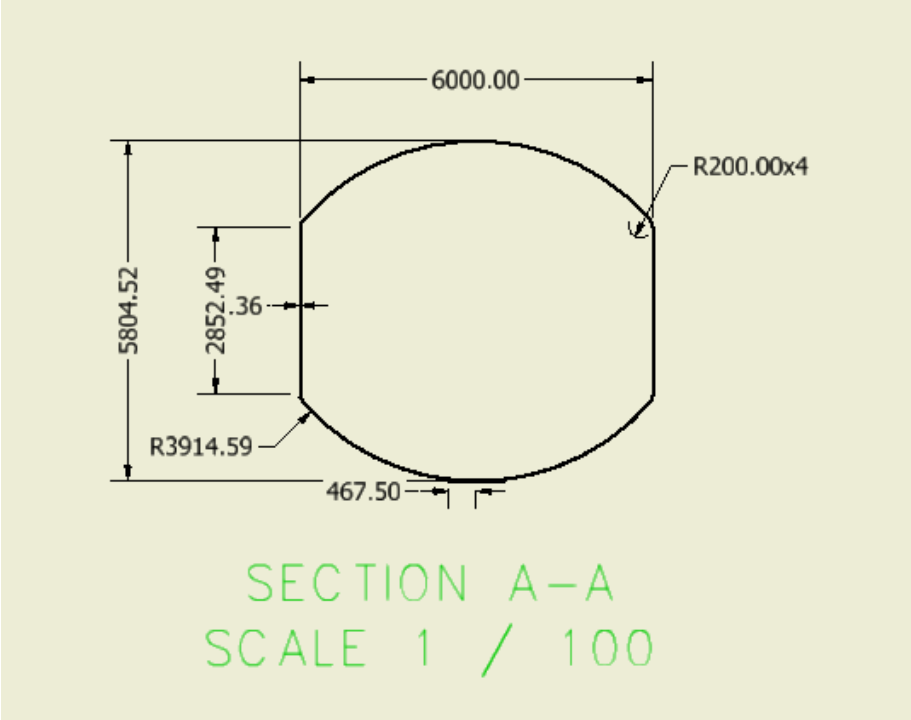

Figure 21: Full Dimensioned Drawing of LH2 Fuel Tank (mm)

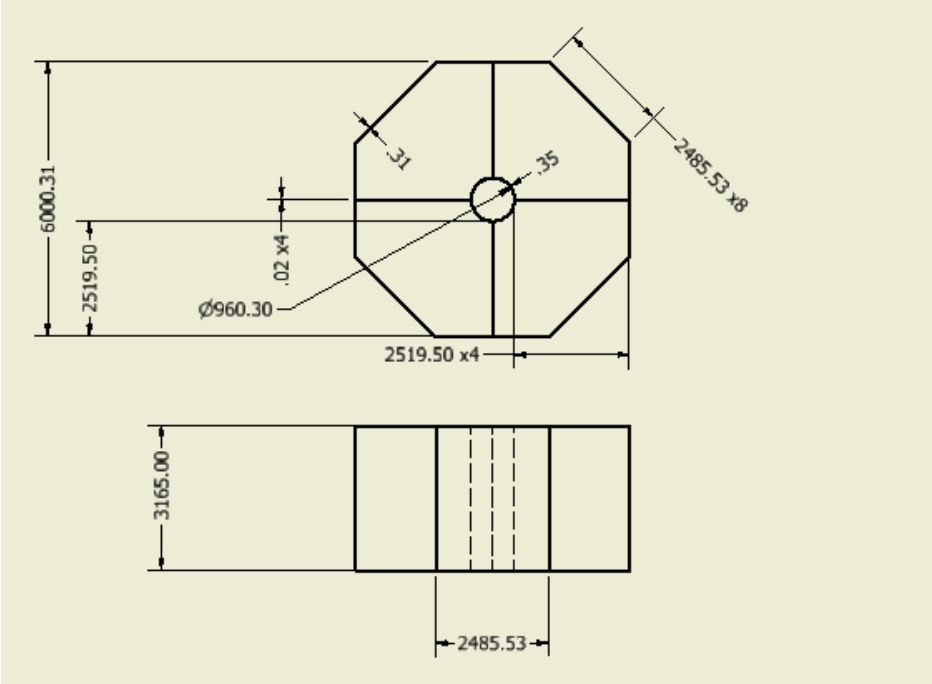

Figure 22: Full Dimensioned Drawing of Octagonal Base (mm)

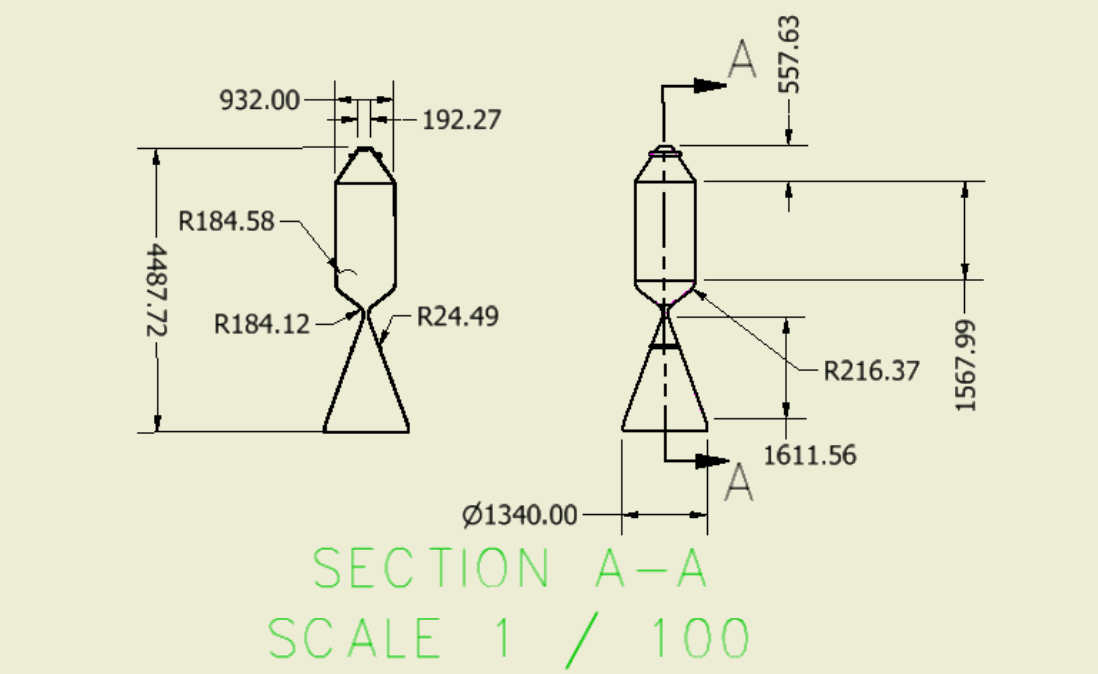

Figure 23: Full Dimensioned Drawing of SNRE (mm)

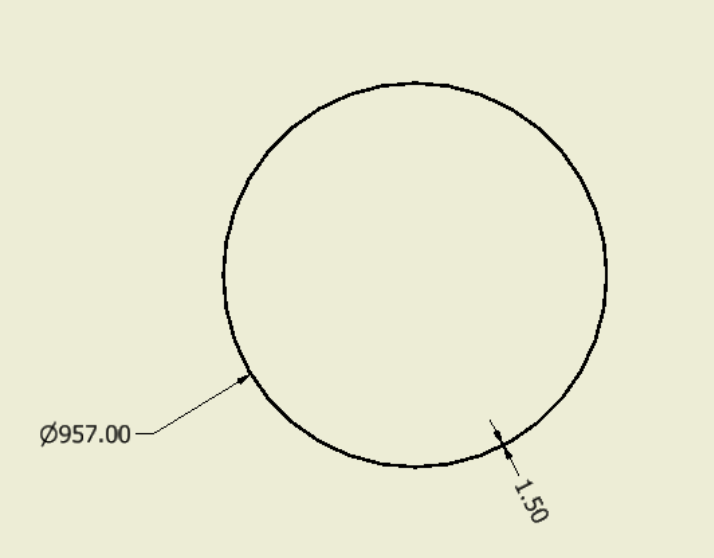

Figure 24: Vertical View of Engine Shaft (mm)

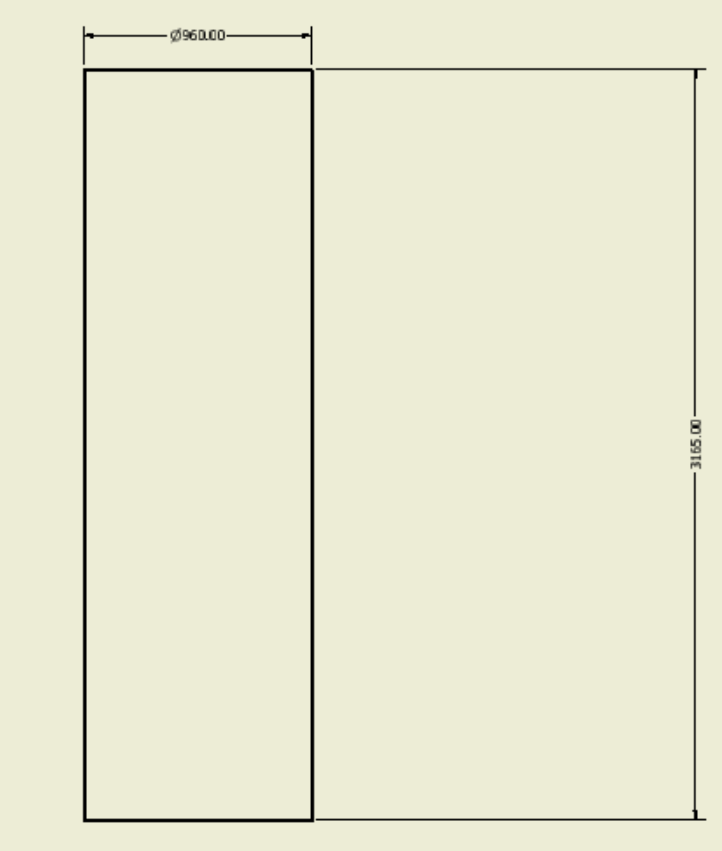

Figure 25: Horizontal View of Engine Shaft (mm)

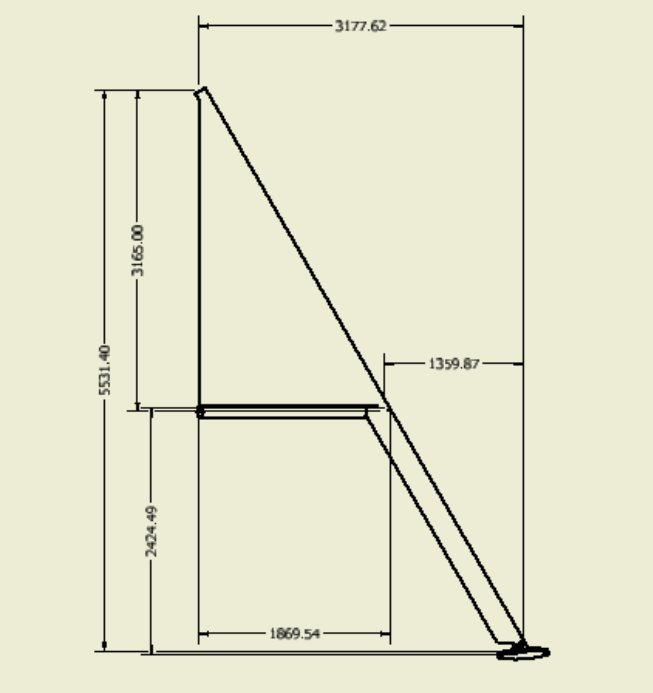

Figure 26: Fully dimensioned schematic of a Landing Leg (mm)

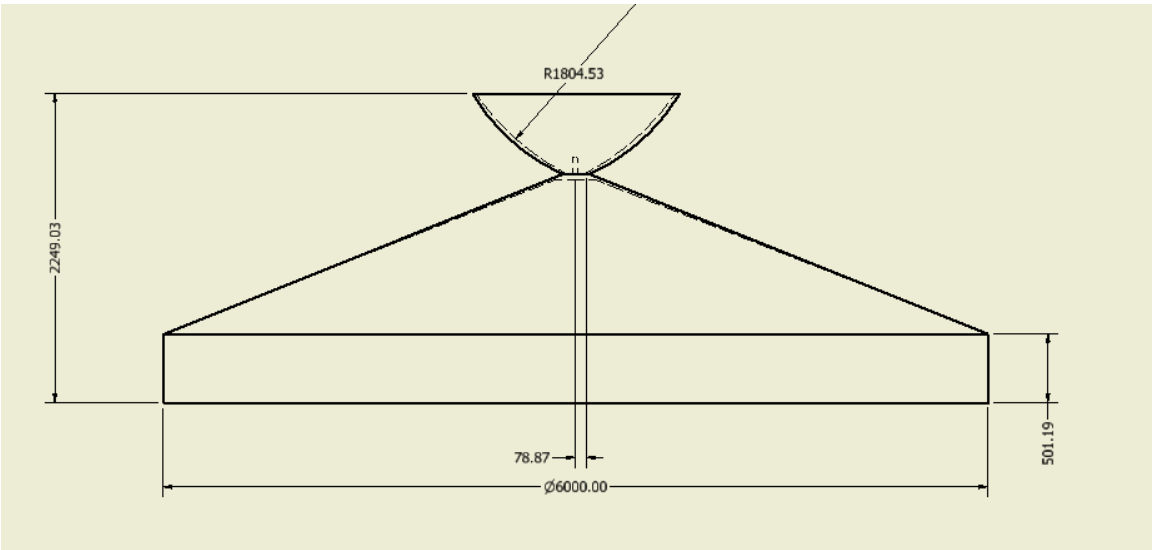

Figure 27: Fully Dimensioned Schematic of GNC and Communications "Hat" (mm)

MATLAB Code

MAIN PROGRAM

```
clc

clear all
close all


%Constant Variables

g=9.81/6; %gravitational acceleration


%    M_empty=4500; %kg, Empty mass based on Apollo Lunar Module Dry Mass
%  M_empty=2500;
    M_empty=2500;

%    T_full=111000; %N, based on the Pewee Engine developed in the 70s that
outputted 111kN of thrust
  T_full=32916;
%     T_full=74290;
%   T_full=71000;

%    isp=940;
   isp=894;
%     isp=900;
%  isp=235;

%     m_dot_full=12.5; %mass flow rate in kg/s
  m_dot_full=3.753;
%      m_dot_full=8.414316;
%  m_dot_full=30.828;

gamma1=45; %degrees

d_impact=0;%intial impact parameter set to 0

x_target=25000;%target distance in meters

s=1; %the intial value of s, allows to program to run the ascent function
first. This feature is in place so the program can known when to run each
function for certain phases of the hop.
t_cutoff=0;%time of milestones for each hop (ascent cutoff)
t_flight=0;
t_hover=0; %when descent accerlation equals 0
t_landing=0; %time of landing
t_reiginite=0; %time of reignition for powered descent
t_end_hop=0;
h_restart=0;
num_hops=0;
```

```
vec_length=length(1.5:0.75:9);

del_t=0.25;
t_end_here=36000;

MR_count=0;
MRcount=0;
loopCount=0;

graph_single_MR=false;

for h_ratio=0.15:0.015:0.99
for MR=1.5:0.375:9 %Chooses the Mass Ratio of a Given Lander, where the
weight filled with fuel is MR*M_empty

    Mi=MR*M_empty;
    Mf=Mi;
    fprintf('MR= %f \n',MR);
    del_t=0.25; %seconds
    num_hops=0;
    indexer=0;
    t_rel=0;
    total_x_distance=0;
    for t=0:del_t:t_end_here;%3600 %this is the main reference time that the
program uses
%
%         fprintf('t= %f \n',t);
        kk=kk+1;
        t_flight=t+t_rel-t_end_hop; %this time variable references where the
vehicle is at a given time

        if s==1

[s,Mf,t_cutoff,dcutoff,hcutoff,Vy_cutoff,h_apogee,Vx,h_rel,Vy,d_impact,t_rel,
t_flight,del_t_ap,landed,crashed,x_counter,indexer,vec_h,vec_x] =
ascent(s,del_t,g,d_impact,m_dot_full,gamma1,T_full,Mf,t_flight,t,x_target,num
_hops,indexer); %ASCENT
        elseif s==1.5
            indexer=indexer+1;
            impact1(indexer)=d_impact;
            impact_dist=impact1(impact1~=0);

[h_restart,gamma2,Vy_reignite,d_restart,t_restart,d,del_t_cutoff2restart] =
coast(s,h_apogee,g,Vy_cutoff,hcutoff,dcutoff,t,t_flight,t_cutoff,Vx,del_t_ap,
h_ratio,num_hops,Mf,Mi,t_rel,del_t);  %COAST
                t_rel=t_rel+del_t;
                h_rel=h_rel-0.5*g*(del_t)^2+Vy*del_t;
                Vy=Vy-g*del_t;
                x_counter=x_counter+Vx*del_t;
                vec_h(indexer)=h_rel;
                vec_x(indexer)=x_counter;
                s=2;
        elseif s==2
            if d==0
            t_rel=t_rel+del_t;
            h_rel=h_rel-0.5*g*(del_t)^2+Vy*del_t;
```

```
            Vy=Vy-g*del_t;
            x_counter=x_counter+Vx*del_t;
            indexer=indexer+1;
            vec_h(indexer)=h_rel;
            vec_x(indexer)=x_counter;

            end


[s,t_landing,num_hops,Mf,t_hover,t_end_hop,h_rel,Vy,d,Vx,t_rel,t_flight,d_imp
act,landed,crashed,x_counter,total_x_distance,vec_h,vec_x] =
descent(s,Vy_reignite,g,del_t,Mf,m_dot_full,t,t_flight,h_rel,Vy,h_restart,num
_hops,Vx,T_full,t_rel,d,x_counter,total_x_distance,indexer,vec_h,vec_x,isp);
%DESCENT

            if landed==1
                if MR<3
                    MRcount=MRcount+1;
                end
                   [C] =
Extract_Data_hops(MR,Mi,Mf,h_apogee,h_restart,x_target,num_hops,landed,crashe
d,s,h_rel,Vy,t_flight,MRcount,loopCount,x_counter,total_x_distance,h_ratio);
                   [fig] = traj_plot(vec_h,vec_x,graph_single_MR);
                loopCount = loopCount + 1;
            end



      if crashed==true && (num_hops>1 && Mf<5000)
%         s=1;
%         num_hops_vec(kk,1)=num_hops;
        if MR<3
            MRcount=MRcount+1;
        end
        %%Changes
         [C] =
Extract_Data_hops(MR,Mi,Mf,h_apogee,h_restart,x_target,num_hops,landed,crashe
d,s,h_rel,Vy,t_flight,MRcount,loopCount,x_counter,total_x_distance,h_ratio);
        loopCount = loopCount + 1;
      end
        disp('MOVING ON TO NEXT MR')
        s=1;
        num_hops_vec(kk,1)=num_hops;
        num_hops=0;
        x_counter=0;
        total_x_distance=0;
        d_impact=0;
%       end

end
end
```

FUNCTIONS:

ASCENT

```
function
[s,Mf,t_cutoff,dcutoff,hcutoff,Vy_cutoff,h_apogee,Vx,h_rel,Vy,d_impact,t_rel,
t_flight,del_t_ap,landed,crashed,x_counter,indexer,vec_h,vec_x] =
ascent(s,del_t,g,d_impact,m_dot_full,gamma1,T_full,Mf,t_flight,t,x_target,num
_hops,indexer)

%This is the ascent function. The primary goal of this function is to
%simulate launch for each hop and determine when to shut off the engine
%when the targeted impact distance is reached by modeling 2D projectile
%motion. A quadratic equation is solved to determine the time of impact and
how far away the impact will be.
%Once the horizontal target is met. The engine will shut off.
Vy=0;
Vx=0;
h_rel=0;

iter=1;
t_cutoff=0;
dcutoff=0;
hcutoff=0;
Vy_cutoff=0;
h_apogee=0;
t_rel=0;
del_t_ap=0;
landed=false;
crashed=false;
x_counter=0;
vec_h=0;
vec_x=0;
 while d_impact<(x_target) %While the impact distance is less than the target
distance
   indexer=indexer+1;
   t_rel=t_rel+del_t;


    Mf=Mf-m_dot_full*del_t; %mass of spacecraft as engine is burning

    %componets of accleration
    %Equations relating to mass and accleration
    a_t=T_full/Mf; %total accerlation

    if T_full<Mf*g

        disp('Vechicle is too heavy: it will not take off')
        disp(' ')
        disp('Number of hops completed: ')
        disp(num_hops)
        s=1;
        h_rel=0;
        Vy=0;
```

```
        TWR=T_full/(Mf*g);
        disp('TWR is: ')
        disp(TWR)
        disp('Mf is: (kg)')
        disp(Mf)
        num_hops=0;
        break
    end

    a_x=T_full/Mf*cosd(gamma1);%x accerlation

    a_y=T_full/Mf*sind(gamma1)-g; %y accerlation

    a_net=sqrt((a_x)^2+(a_y)^2); %net accerlation

    if a_y<0

        disp('Y accerlation is negative: either increase gamma or waste fuel
until your Y accleration is greater than 0')
        disp(' ')
        disp('Number of hops completed: ')
        disp(num_hops)
        s=1;
        h_rel=0;
        Vy=0;
        TWR=T_full/(Mf*g);
        disp('TWR is: ')
        disp(TWR)
        disp('Mf is: (kg)')
        disp(Mf)
        num_hops=0;
        break
    end

    %---------------------------------------

   %Kinematic Equations



%    Vy=Vy+a_y*del_t; %Vertical Velocity
%
%    Vx=Vx+a_x*del_t;  %Horizontal Velocity

   h_rel=h_rel+0.5*a_y*del_t.^2+Vy*del_t; %Vertical distance

   x_counter=x_counter+0.5*a_x*del_t.^2+Vx*del_t; %Horizontal distance

   Vy=Vy+a_y*del_t; %Vertical Velocity

   Vx=Vx+a_x*del_t;

   vec_h(indexer)=h_rel;
   vec_x(indexer)=x_counter;
```

```
    %-----------------------------------------------------

   del_t_ap=Vy/g; %time it takes to reach apogee (assuming engine is cutoff)
   del_t_target=sqrt(2*h_apogee/g);
   h_apogee=h_rel+Vy*del_t_ap-0.5*g*del_t_ap^2; %current apogee if engine
cuts off

%     d_apogee=Vx*(t_flight+t_ap); %horizontal distance from launch site

    %-----------------------------------------------------
    %Solve the quadratic equation to determine the time of impact
    %and the corresponding distance traveled. When the engine is
    %shutoff we can model the spacecraft via projectile motion

   del_t_impact=del_t_ap+del_t_target;
   d_impact=(del_t_impact*Vx)+x_counter; % using t_impact we solve for the
impact distance



    %Possibly REDUNDANT if statement

    if d_impact>=x_target %(if we reach our target impact distance)
%
%         disp(t)
%         disp(t_flight)
%         disp('the time is above')
%         disp(' ')
%         fprintf('x_target %f \n',x_target);
%         fprintf('d_impact %f \n',d_impact);
        t_cutoff=t_rel; %mark the time of ascent cutoff

        dcutoff=x_counter; %distance relative to the launchsite is noted
where engine cutoff occurs

        Vy_cutoff=Vy; %Vertical velocity componet at time of engine cutoff

        hcutoff=h_rel;  %altitude of engine cutoff

        Mf_cutoff_ascent=Mf; %final mass after ascent cutoff for hop
        t_flight=t_flight+t_rel;

        s=1.5;  %the value of s notifies that the hop has completed a certain
phase. By this point the ascent is completed and the program can continue to
the coast function.

        %IMPORTANT: figure out a way to #hops and fuel data
        disp(' ')
        disp('Ascent Program complete')
        disp(' ')
%         disp('The apogee is (m): ')
%         disp(h_apogee)
        disp(' ')
```

```
%         break

    else

%         continue
    end



    if Mf<2500 %This if statement will end the program if the engine is out
of fuel. The dry mass is 4400 kg

        disp('The engine is out of fuel and will crash.')
        disp('Ran out of fuel during Ascent:')
        disp(' ')
%         disp('ALTITUDE: ')
%         disp(h_rel)
%         disp('km')
        crashed=true;
%         disp('Vertical Velocity: ')
%         disp(Vy)
%         disp('m/s')
        s=-1; %value of s changes to s so the program will not continue to
subsequent functions
        disp(' ')
        disp('Number of completed hops: ')
        disp(num_hops) %display number of hops
        disp(' ')
        t_flight=t_flight+t_rel;

        break

    else

%         continue

    end



end
```

COAST

```
function
[h_restart,gamma2,Vy_reignite,d_restart,t_restart,d,del_t_cutoff2restart] =
coast(s,h_apogee,g,Vy_cutoff,hcutoff,dcutoff,t,t_flight,t_cutoff,Vx,del_t_ap,
h_ratio,num_hops,Mf,Mi,t_rel,del_t)

%This is the coast function. For each hop there will be a significant
%period of where the engine will be off and the spacecraft will be in
freefall. The objective of this function is
```

```
%to calculate when to reignite the engine for powered descent, the altitude
and horizontal distance relative to the launch site
%to calculate the flight path angle for powered descent and the vertical
velocity when the descent sequence begins.
%Unlike the other two functions there is no iterative process. This
%function serves as a calculator.

  t_rel=t_rel+del_t;
  h_restart=h_ratio*h_apogee; %right now percent is arbitrary
disp('Altitude of Apolune is: (m) ')
disp(h_apogee)
disp(' ')
disp('Altitude of restart altitude is: (m) ')
disp(h_restart)
%Calculation of parameters at start time of ignition


del_t_ap2restart=sqrt((h_apogee-h_restart)/(2*g));

% disp(h_apogee)
% disp(h_restart)
% disp(del_t_ap)
% disp('s')
% disp(del_t_ap2restart)
% disp('s')
del_t_cutoff2restart=del_t_ap2restart+del_t_ap;

% disp(del_t_cutoff2restart)
%ensure t_restart is a postive real interger (also verify if you need to add
t_flight)
%Verify relationship with
%t/t_flight

deltaV=g*(del_t_cutoff2restart);
% disp(deltaV)
% disp('m/s')

Vy_reignite=Vy_cutoff-deltaV; %Y componet of velocity for intial conditions
for powered descent (should be a negative value)
% disp(' ')
% disp('Vy_reignite')
% disp(Vy_reignite)


%ASSUME constant Vx

gamma2=atand(Vy_reignite/Vx); %find new flight path angle when powered
descent begins (verify if you need to add or subtract 180 degrees)

% t_coast=t_cutoff-t_restart; %VERIFY

d_restart=dcutoff+Vx*(del_t_cutoff2restart); %horizontal distance covered
when engine is restarting
t_restart=t_rel+del_t_cutoff2restart;
```

```
%VERIFY

%FIGURE OUT IF THIS IS CORRECT PLACEMENT
s=2;

 disp(' ')
 disp('Coast Calculation complete')
 disp(' ')
 d=0;

end

%end
```

DESCENT

```
function
[s,t_landing,num_hops,Mf,t_hover,t_end_hop,h_rel,Vy,d,Vx,t_rel,t_flight,d_imp
act,landed,crashed,x_counter,total_x_distance,vec_h,vec_x] =
descent(s,Vy_reignite,g,del_t,Mf,m_dot_full,t,t_flight,h_rel,Vy,h_restart,num
_hops,Vx,T_full,t_rel,d,x_counter,total_x_distance,indexer,vec_h,vec_x,isp)

%This is the descent function. The primary purpose of this function is
%monitor the powered descent of the spacecraft. This iterative has several
%if-statements to categorize the descent into 3 phases: intial burn,
%vertical burn with accerlation, and the final approach which has no
%accerlation.

% h=hcutoff-0.5*g*(t_restart-t_cutoff)^2+Vy*(t-t_cutoff);
%VERIFY Vy_reignite and h_reginite match up
iter1=0;
t_landing=0;
t_hover=0.0;
t_end_hop=0.0;
m_dot_low=0;
%%%%%%%%%%%%%%%%%%%%%%%%%%%%%%%%%%%%%%%%%%%%%%%%%%%%%%%%%%%%%%%%%%%%%%%%%%%
d_impact=25000;
%%%%%%%%%%%%%%%%%%%%%%%%%%%%%%%%%%%%%%%%%%%%%%%%%%%%%%%%%%%%%%%%%%%%%%%%%%%
crashed=false;
landed=false;
x_landing=0;
disp(t_rel)

while h_rel<h_restart && s==2 && Vy<0
 d=1;


 Vy_restart=Vy;


if Vx>0.5  %Phase I: Intial Retrograde Burn at Full Throttle

        %         del_t_engine=t-t_restart; %the change in time used for the
engine
```

```
        Mf=Mf-(del_t)*m_dot_full; %equation monitoring the change of mass

        a=T_full/(Mf); %the total accerlation
        gamma2=atand(Vy/Vx);
        x_counter=x_counter+Vx*del_t+a*cosd(gamma2+180)*del_t^2;

%
        h_rel=h_rel+0.5*(-g+a*sind(gamma2+180))*del_t^2+Vy*del_t;

         Vx=Vx+a*cosd(gamma2+180)*del_t;
         Vy=Vy-g*del_t+a*sind(gamma2+180)*del_t;
%         vec_h(t)=h_rel;
%         vec_x(t)=x_counter;

        %the flight path angle will change as Vx decreases
        t_rel=t_rel+del_t;
        t_flight=t_flight+t_rel;
        indexer=indexer+1;
        vec_h(indexer)=h_rel;
        vec_x(indexer)=x_counter;

         if Vy>-0.5
            Vy=-2;

         end

         if Vx<=-0.5
            Vx=0;

         end
         if  Vy<-5 && h_rel<5

                        disp('The Vehicle has hit the surface too fast: it
has crashed')
                         landed=false;
                         crashed=true;
                        disp('Horizontal Velocity (m/s):')
                        disp(Vx)
                        disp('m/s')
                        disp('Vertical Velocity (m/s):')
                        disp(Vy)
                        disp('m/s')
                        s=-1; %display number of hops
                        disp(' ')
                        disp('Number of hops completed: ')
                        disp(num_hops)

                        t_rel=0;
                        break
         end
%%%%%%%%%%%%%%%%%%%%%%%%%%%%%%%%%%%%%%%%%%%%%%%%%%%%%%%%%%%%%%%%%%%%%%%
             if Mf<2500
%%%%%%%%%%%%%%%%%%%%%%%%%%%%%%%%%%%%%%%%%%%%%%%%%%%%%%%%%%%%%%%%%%%%%%%
                disp('The engine is out of fuel and will crash.')
```

```
                disp(' ')
                disp('Vehicle crashed during Descent: ')
                disp(' ')
                disp('ALTITUDE: ')
                disp(h_rel)
                disp('m')
                landed=false;
                crashed=true;
                disp('Vertical Velocity: ')
                disp(Vy)
                disp('m/s')

                 s=-1; %display number of hops
                 disp(' ')
                 disp('Number of hops completed: ')
                 disp(num_hops)

                break
             end

    elseif Vx<=0.5 && Vy<-5  %Phase 2: Vertical Flight with accerlation in


            Vx=0; %manually set Vx to 0 zero once it is close enough
            disp(' ')
            ax=0;  %no accleration in x-direction

            Mf=Mf-del_t*m_dot_full;

            ay=T_full/(Mf);



%             Vy=Vy-g*del_t+ay*del_t;
            x_counter=x_counter+Vx*del_t;

%             disp(Vy)
%             disp('m/s')
            h_rel=h_rel+0.5*(-g+ay)*del_t^2+Vy*del_t;

            Vy=Vy-g*del_t+ay*del_t;


            t_rel=t_rel+del_t;
            t_flight=t_flight+t_rel;
            indexer=indexer+1;
            vec_h(indexer)=h_rel;
            vec_x(indexer)=x_counter;
            if Vy>-0.5
            Vy=-2;

            end

            if Vx<=-0.5
```

```
              Vx=0;

            end
            if  Vy<-5 && h_rel<5

                        disp('The Vehicle has hit the surface too fast: it
has crashed')
                         landed=false;
                         crashed=true;
                         disp('Horizontal Velocity (m/s):')
                        disp(Vx)
                        disp('m/s')
                        disp('Vertical Velocity (m/s):')
                        disp(Vy)
                        disp('m/s')
                        s=-1; %display number of hops
                        disp(' ')
                        disp('Number of hops completed: ')
                        disp(num_hops)

                        t_rel=0;
                        break
            end

%%%%%%%%%%%%%%%%%%%%%%%%%%%%%%%%%%%%%%%%%%%%%%%%%%%%%%%%%%%%%%%%%%%%%%%%%%%%
            if Mf<2500
%%%%%%%%%%%%%%%%%%%%%%%%%%%%%%%%%%%%%%%%%%%%%%%%%%%%%%%%%%%%%%%%%%%%%%%%%%%%
                disp('The engine is out of fuel and will crash.')
                disp(' ')
                disp('Vehicle crashed during Descent: ')
                disp(' ')
                disp('ALTITUDE: ')
                disp(h_rel)
                disp('m')
                landed=false;
                crashed=true;
                disp('Vertical Velocity: ')
                disp(Vy)
                disp('m/s')

                 s=-1; %display number of hops
                 disp(' ')
                 disp('Number of hops completed: ')
                 disp(num_hops)

                break
            end

else
%           disp('Phase III executes: ')
            Vx=0;
            Vy=-2;
            x_counter=x_counter+Vx*del_t;

            if  Vy<-5 && h_rel<5
```

```
                        disp('The Vehicle has hit the surface too fast: it
has crashed')
                         landed=false;
                         crashed=true;
                        disp(' ')
                    disp('Horizontal Velocity (m/s):')
                    disp(Vx)
                    disp('m/s')
                    disp('Vertical Velocity (m/s):')
                    disp(Vy)
                    disp('m/s')
                        s=-1; %display number of hops
                        disp(' ')
                        disp('Number of hops completed: ')
                        disp(num_hops)

                        t_rel=0;
                        break
             end
%%%%%%%%%%%%%%%%%%%%%%%%%%%%%%%%%%%%%%%%%%%%%%%%%%%%
            if Mf<2500
%%%%%%%%%%%%%%%%%%%%%%%%%%%%%%%%%%%%%%%%%%%%%%%%%%%%
             disp('The engine is out of fuel and will crash.')
             disp(' ')
             disp('Vehicle crashed during Descent: ')
             disp(' ')
             disp('ALTITUDE: ')
             disp(h_rel)
             disp('m')
             landed=false;
             crashed=true;
             disp('Vertical Velocity: ')
             disp(Vy)
             disp('m/s')

             s=-1; %display number of hops
             disp(' ')
             disp('Number of hops completed: ')
             disp(num_hops)

             break

            end

        %Phase 3: Vertical flight with no acceleration
%
%
%               disp('REMAINING MASS: ')
%               disp(' ')
%               disp(Mf)
%               disp('kg')
%               disp(m_dot_low)
%               disp('kg/s')
%                 disp(h_rel)
%                 disp(' ')
```

```
                %                   %Thrust=Weight
                %
                %                   %T=m_dot*Ve

                t_hover=t;



                Ve=(isp*9.81)*0.9475;

                W=Mf*g;

                m_dot_low=W/Ve;

                Mf=Mf-(del_t)*m_dot_low;

                ax=0;

                ay=-g;

                t_rel=t_rel+del_t;
                h_rel=h_rel+Vy*del_t;
                t_flight=t_flight+t_rel;
                indexer=indexer+1;
                vec_h(indexer)=h_rel;
                vec_x(indexer)=x_counter;
%

%%%%%%%%%%%%%%%%%%%%%%%%%%%%%%%%%%%%%%%%%%%%%%%%%%%%%%%%%%%%%%%%%%%%%%%%%%%%%%%
             if h_rel<5 && Mf>2500 && Vy==-2 && Vx==0 %nested if-statement to
determin when the veihicle touches down
%%%%%%%%%%%%%%%%%%%%%%%%%%%%%%%%%%%%%%%%%%%%%%%%%%%%%%%%%%%%%%%%%%%%%%%%%%%%%%%
                    disp('Vehicle has landed')
                    landed = true;


                    s=1; %the landing function has been sucesfully executed,
now the program can begin the ascent function assuming there is still fuel
on-board

                    t_landing=t_flight+t_rel; %time of landing noted

                    disp('Remaining fuel in (kg): ')

                    disp(' ')

                    disp(Mf-3500);
                    disp(' ');

                    disp('Number of hops completed: ')
                    d_impact=0;
                    disp(' ')
```

```
                    num_hops=num_hops+1; %number of hops counted
                    disp(num_hops)

                    t_end_hop=t_rel;
                    t_rel=0;

                    total_x_distance=total_x_distance+x_counter;
                    t_flight=t_flight+t_rel;

            end


end




end
end
```

TRAJECTORY PLOTTING

```
function [fig] = traj_plot(vec_h,vec_x,graph_single_MR)
fig=0;
if graph_single_MR==true

   fig=1;

   plot(vec_x,vec_h)
  hold on
title('Trajectory Plot: MR = 1.5')
xlabel('Horizontal Distance (meters) ')
ylabel('Altitude (meters) ')
 axis tight
hAx = gca;             % handle to current axes
hAx.YAxis.Exponent=0;  % don't use exponent
hAx.XAxis.Exponent=0;
legend


end



end
```

References

Lunar Rocks and Soils from Apollo Missions. (n.d.). Retrieved from https://curator.jsc.nasa.gov/lunar/.

Apollo Traverses on Earth. (n.d.).Retrieved from https://www.hq.nasa.gov/alsj/TraverseMapsEarth.html.

Heiken, G., Vaniman, D., French, B. M., & Vaniman, D. T. (1991). *The Lunar sourcebook: a users guide to the moon*. Cambridge: Cambridge University Press.

Zacny, K. (2012). Lunar Drilling, Excavation and Mining in Support of Science, Exploration, Construction, and In Situ Resource Utilization (ISRU). *Moon*, 235–265. doi: 10.1007/978-3-642-27969-0_10

Spudis, P. D. (2013, April 8). The Mystery of Shackleton Crater. Retrieved from https://www.airspacemag.com/daily-planet/the-mystery-of-shackleton-crater-17072957/.

Barnatt, C. (2016, 30 January) Retrieved from https://www.explainingthefuture.com/helium3.html.

Baker, D. (2019). *Nasa moon missions operations manual: 1969-1972 (Apollo 12, 14, 15, 16 and 17): an insight into the engineering, technology and operation of NASAs advanced lunar flights*. Sparkford: Haynes Publishing.

Summary. (2019, September 9). Retrieved from https://mars.nasa.gov/msl/spacecraft/instruments/summary/.

Mohon, L. (2017, August 2). New NASA Contract Will Advance Nuclear Thermal Propulsion Technology. Retrieved from https://www.nasa.gov/centers/marshall/news/news/releases/2017/nasa-contracts-with-bwxt-nuclear-energy-to-advance-nuclear-thermal-propulsion-technology.html.

(n.d.). Retrieved from http://asm.matweb.com/search/SpecificMaterial.asp?bassnum=MA7075T6.

Dave, D. (2015, August 12). Propulsion. Retrieved from https://www.slideshare.net/deepdave3/propulsion-51552822

Sutton, G. P., & Biblarz, O. (2017). *Rocket propulsion elements*. Hoboken (N.Y.): Wiley.

Belair, M. L., Sarmiento, C., & Lavelle, T. (2013). Nuclear Thermal Rocket Simulation in NPSS. *49th AIAA/ASME/SAE/ASEE Joint Propulsion Conference*. doi: 10.2514/6.2013-4001

Anon. (2018, March 9). LEU NTP, NASA's New Nuclear Rocket – Part 1: Where We've Been Before. Retrieved from https://beyondnerva.com/2017/12/15/leu-ntp-nasas-new-nuclear-rocket-part-1-where-weve-been-before/.

ENGINE LIST 2. (n.d.). Retrieved from http://www.projectrho.com/public_html/rocket/enginelist2.php#snre.

Borowski, S. (n.d.). Affordable Development and Demonstration of a Small NTR ... Retrieved from https://ntrs.nasa.gov/archive/nasa/casi.ntrs.nasa.gov/20150023036.pdf.

Borowski, S. K., & McCurdy, D. R. NTR Performance Parameters for Science, Cargo Delivery and Crewed Exploration Missions., NTR Performance Parameters for Science, Cargo Delivery and Crewed Exploration Missions. (n.d.).

New Glenn. (n.d.). Retrieved from https://www.blueorigin.com/new-glenn/.

Spacexcmsadmin. (2019, September 28). Starship. Retrieved from https://www.spacex.com/starship.

Flight Performance of Atlas-Centaur AC-13, AC-14, AC-15 in support of the Surveyor Lunar Landing Program, Flight Performance of Atlas-Centaur AC-13, AC-14, AC-15 in support of the Surveyor Lunar Landing Program (n.d.). Cleveland, OH.

Zheng, H., Zeng, X., Zhang, J., & Sun, H. (2018). The Application of Carbon Fiber Composites in Cryotank. *Solidification*. doi: 10.5772/intechopen.73127

Weiss, S. P. Apollo experience report: lunar module structural subsystem, Apollo experience report: lunar module structural subsystem (1973). Washington, D.C.: National Aeronautics and Space Administration.

WEIXIONG, R. H. (2017). *Preliminary Design Of Reusable Lunar Lander Landing System* (dissertation).

spacecraft.ssl.umd.edu Dave Akin's Web Site. (n.d.). Retrieved from https://spacecraft.ssl.umd.edu/.

Leve, F. A. (2009). *Development of the Spacecraft Orientation Buoyancy Experimental Kiosk* (dissertation).

Jones, B. (2017, October 13). NASA's new ion thruster breaks records, could take humans to Mars. Retrieved from https://futurism.com/nasas-new-ion-thruster-breaks-records-could-take-humans-to-mars.

(n.d.). Retrieved from http://heroicrelics.org/info/lm/lm-evolution.html.

BWX Technologies, Inc.: People Strong, Innovation Driven. (n.d.). Retrieved from https://www.bwxt.com/what-we-do/nuclear-thermal-propulsion-ntp.

Larson, W. J. (1997). *Space mission analysis and design*. Torrance, CA: Microcosm.

Chen, W.-H., Wu, P.-H., Wang, X.-D., & Lin, Y.-L. (2016). Power output and efficiency of a thermoelectric generator under temperature control

Crain, T., Bishop, R. H., Carson, J. M., Trawny, N., Sullivan, J., Christian, J. A., … Hanak, C. (2016). Approach-Phase Precision Landing with Hazard Relative Navigation: Terrestrial Test Campaign Results of the Morpheus/ALHAT Project. *AIAA Guidance, Navigation, and Control Conference*. doi: 10.2514/6.2016-0099

Carson, J. M., Seubert, C., Amzajerdian, F., Bergh, C., Kourchians, A., Restrepo, C., … Garcia, R. (2017). COBALT: Development of a Platform to Flight Test Lander GN&C Technologies on Suborbital Rockets. *AIAA Guidance, Navigation, and Control Conference*. doi: 10.2514/6.2017-1496

Chen, W.-H., Wu, P.-H., Wang, X.-D., & Lin, Y.-L. (2016). Power output and efficiency of a thermoelectric generator under temperature control. *Energy Conversion and Management*, *127*, 404–415. doi: 10.1016/j.enconman.2016.09.039

Hurlbert, Eric (2019, July). Personal interview.